COMBINED TOTAL STORM TIDE FREQUENCY ANALYSIS FOR SARASOTA COUNTY, FLORIDA

By

R. G. Dean
T. Y. Chiu
S. Y. Wang

Sponsored By

Division of Beaches and Shores
Department of Natural Resources

Submitted By

Beaches and Shores Resource Center
Institute of Science and Public Affairs
Florida State University
Tallahassee, Florida 32306

August, 1988

Table of Contents

List of Figures

Figure		Page

List of Tables

I. INTRODUCTION

1.1 Background

In accordance with the objectives and rationale of the Florida Coastal Construction Control Line, the establishment of the line is based on the damage potential of low frequency (100 year) storms. This necessitates the determination of combined total tides including storm surges, astronomical tide and dynamic wave set-up which occurs primarily inside the wave breaking zone. The objective of the present study, which is carried out for Sarasota County, Florida, is to develop, through numerical modeling, valid estimates of the combined total storm tides for return periods of 10, 50, 100, 200 and 500 years.

1.2 Location and General Description of the Study Area

Figure 1 shows the general location of the study area which consists of coastal zones of all or parts of five barrier islands and a section of the mainland, having a total of about 35 miles of Gulf shoreline. From north to south, the islands are the southern half of Longboat Key, Lido Key (formerly Cerol Isles), Siesta Key, Casey Key, a four-mile section of the mainland and the northern 3/4 of Manasota Key (a peninsula). The keys are intervened by New Pass, Big Sarasota Pass, Midnight Pass (closed in 1983), and Venice Inlet (Casey Pass) and separated from the mainland by Sarasota Bay, Roberts Bay, Little Sarasota Bay, Blackburn Bay and Lemon Bay. The locality is shown on NOAA's Nautical Charts Nos. 11006, 11400, 11408, 11409, 11412 11420, 11424, 11426, 11427 and 11429.

The width of the barrier islands vary from 100 ft. to 1.3 miles with natural ground elevations generally under 10 ft. The beaches of Sarasota County are composed of fine quartz sand and shell fragments with an average around

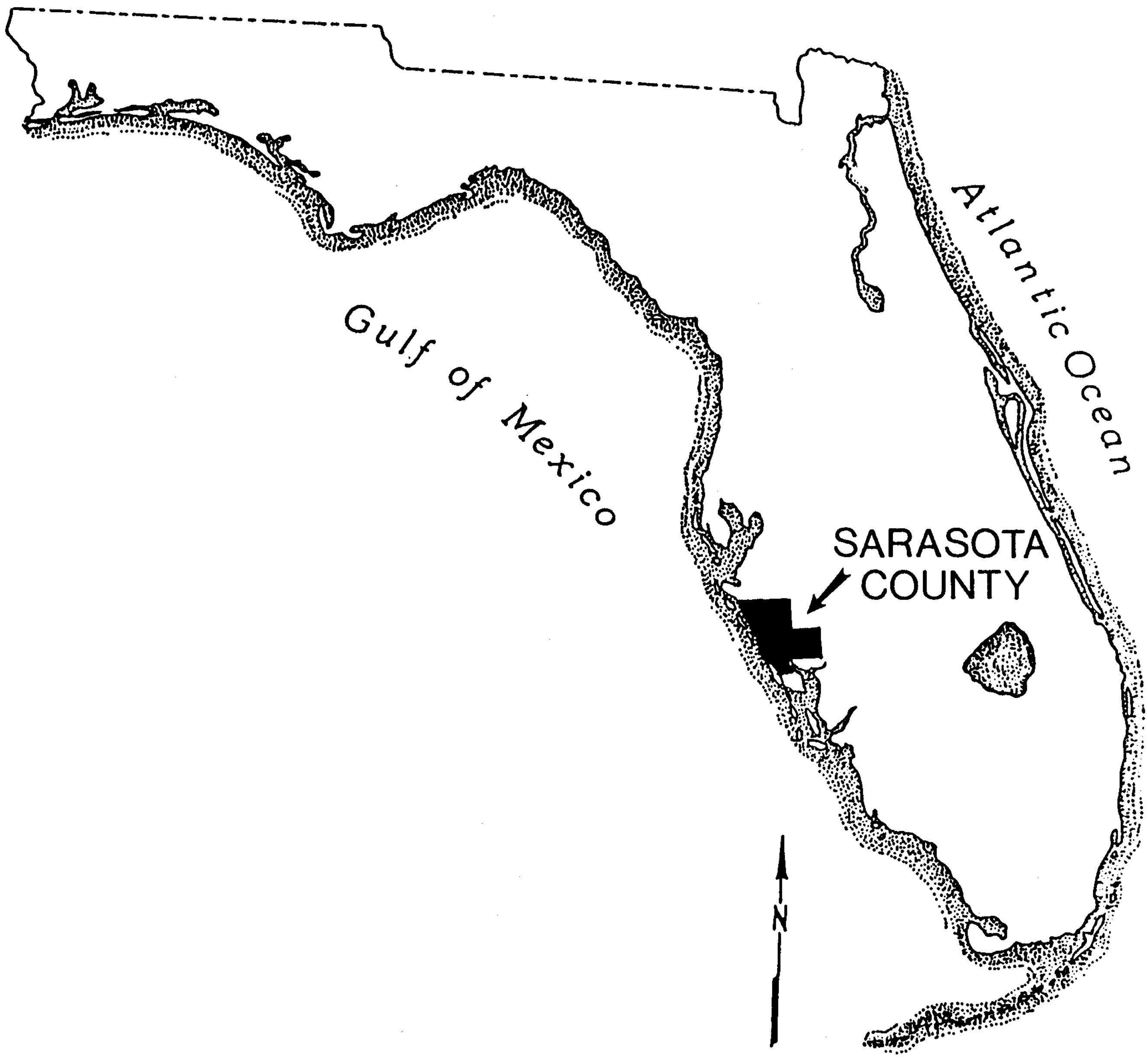

Figure 1 General Location of the Study Area

100 ft. in width. Erosion has been a historical problem.

The reader is referred to References (1)* and (2) for more detailed description of the study area.

1.3 Scope of the Study

The objective of the study is to develop, verify and apply a procedure which will yield valid estimates of the combined total storm tides for various return periods at the vicinity of the shoreline in Sarasota County. Throughout this report, "combined total storm tide" denotes the storm surge due to astronomical tide, wind stress and barometric pressure effects combined with the dynamic wave set-up, the latter occurring dominantly within the wave breaking zone. Available historical hurricane statistics are combined with a set of numerical models to simulate the storm tides at the site of interest. Tidal recordings during hurricanes of September 1947 and June 1966 are employed for model calibration. Friction characteristics for various types of vegetation, buildings and underwater areas are developed to represent the actual variation of friction in the model. A simple one-dimensional model is calibrated and used to reduce the cost of computations for a large number of runs simulating a 2,000 year duration of storm tides. The dynamic wave set-up is based on analytical studies and wave tank tests.

---

*Numbers in parentheses indicate the references listed at the end of this report.

II. HISTORICAL PROBABILITIES OF HURRICANE CHARACTERISTICS IN THE AREA OF INTEREST

2.1 Introduction and Data Source

For purposes of calculating the storm tides that occur during a long period, it is necessary to use realistic statistical representations of the important hurricane parameters: p_O (= central pressure), R (= radius to maximum winds), V_F (= forward speed), θ (= hurricane translation direction) and landfall or alongshore characteristics. The statistical parameters are based on historical hurricane data as presented in References (3). In brief, the empirical cumulative probability distributions are plotted for each of the parameters of interest and are then approximated by a series of straight line segments for computer application. All of the parameters are considered to be independent. The following subsections describe the statistical characteristics of the individual parameters of interest.

2.2 Hurricane Frequency and Direction

The hurricanes causing appreciable storm tides in the vicinity of the Sarasota County shoreline are classified as "landfalling", "alongshore" or "exiting" hurricanes. Reasonably good data are available describing the characteristics of these hurricanes, from 1900 to 1978. For purposes of this report, the data contained in References (3) and (4) are merged for a 300 n.mi. segment of the coast comprising the Sarasota County coastline. The hurricane direction is defined here as the azimuth of hurricane translation direction at the time of landfall, or, if an alongshore hurricane, when in close proximity to the site.

The designation of a hurricane as "landfalling", "alongshore" or "exiting" is somewhat arbitrary as hurricanes travel over a continuous range of directions and there is not a particular direction relative to the shoreline for which the storm tide generating characteristics change markedly. Moreover, the one directional distribution (Figure 2) is applied for all three types of hurricanes. It is important to note that the manner in which the track of a hurricane is characterized for the purposes of this study is different for landfalling, alongshore and exiting hurricanes. For landfalling and exiting hurricanes, the track is specified by a location of landfall (or exit) and track direction, whereas for the alongshore hurricanes, the track is specified by an offshore distance and a track direction (see Section 2.5). Figure 3 presents a definition sketch of the three types of hurricanes.

For purposes of this study, landfalling and exiting hurricanes are considered to be of possible significance if they made landfall within a 300 n.mi. segment of the coast comprising the study area. This segment is extended 150 n.mi. north and 150 n.mi. south from the midpoint of the Sarasota County shoreline. Accordingly, there are 12 landfalling hurricanes, 4 alongshore hurricanes and 9 exiting hurricanes. Figure 4 shows the sectors of propagation paths for the three types of hurricanes and Table AI in Appendix A list all the hurricanes used in this study.

For purposes of computer use, the cumulative probability distribution of hurricane track direction (θ_N) is developed from Figure 2 and is presented in Figure 5.

Based on historical data, it is expected that within a 2,000 year period a total of 633 hurricanes will occur within a distance of 300 n.mi. Of the 633 hurricanes, 304 will be landfalling, 101 alongshore and 228 exiting as represented by percentage distribution in Figure 5.

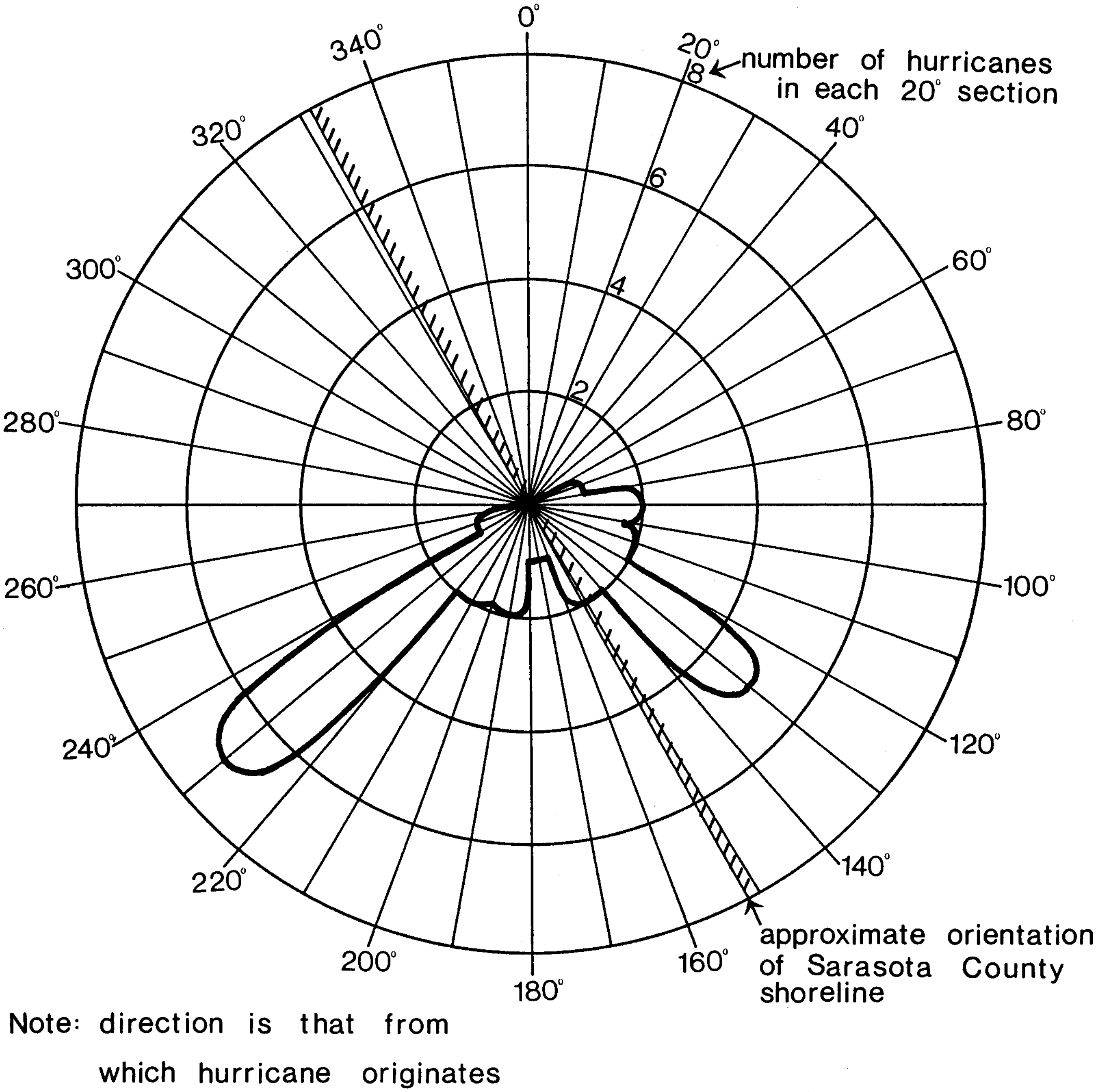

Figure 2 Directional Distribution of Historical Hurricanes in a 300 n.mi. Segment of the Coast Centered at Mid-location of the Sarasota County Coastline

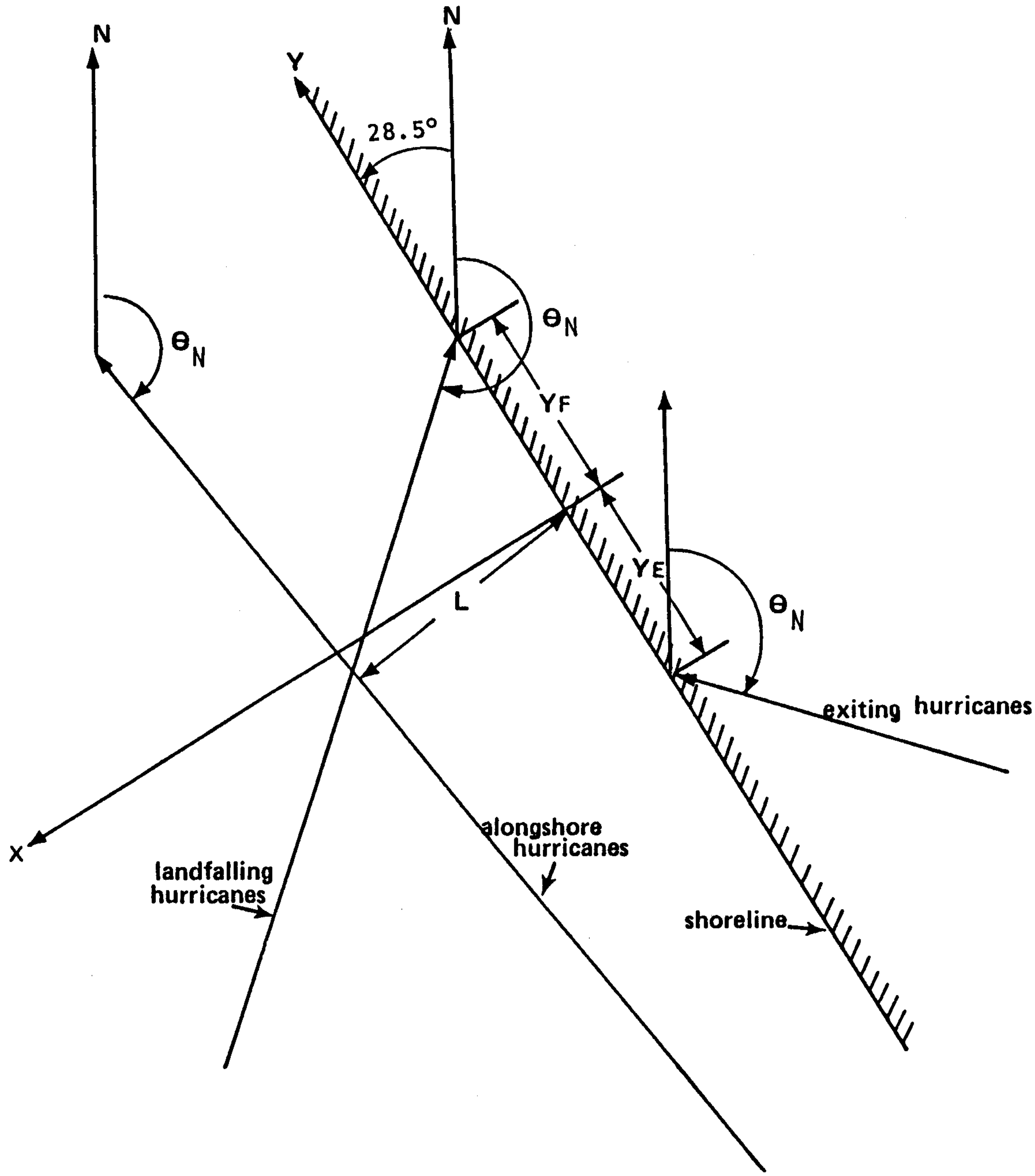

Figure 3 A Definition Sketch of Three Types of Storms

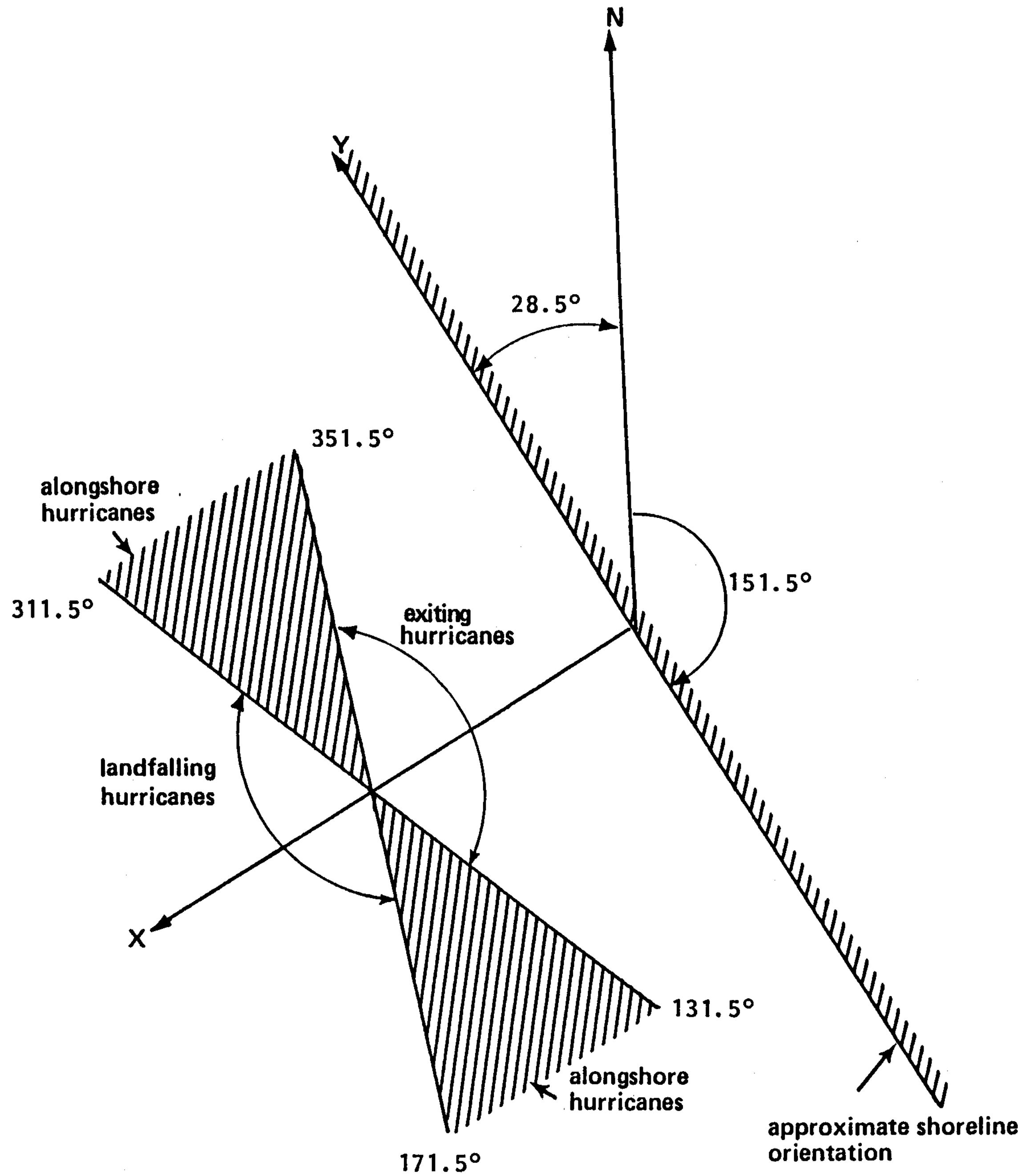

Figure 4 Designation of Landfalling, Alongshore and Exiting Hurricanes Depending on Track Directions Relative to Shoreline Orientation

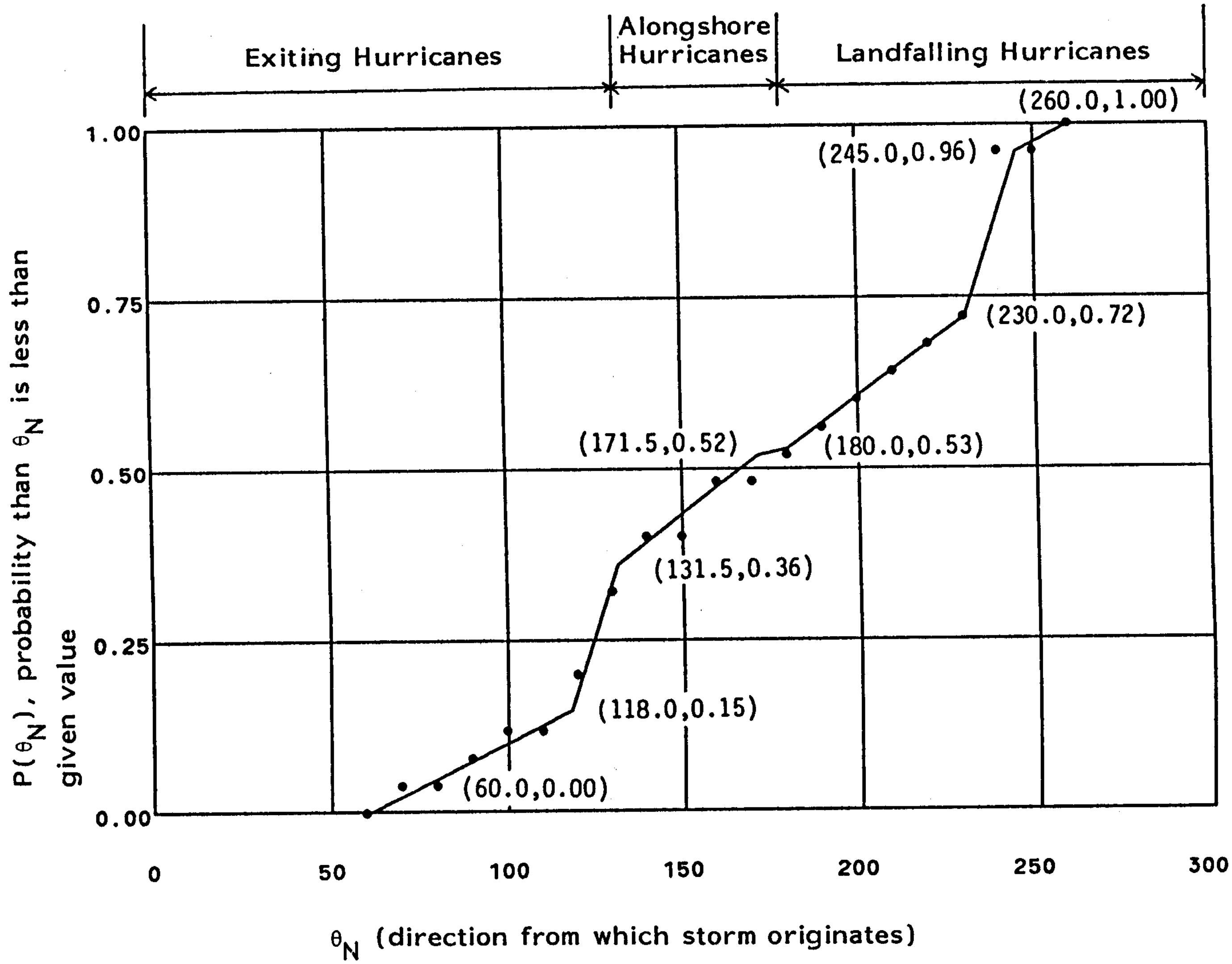

Figure 5 Cumulative Probability Distribution of Hurricane Track Direction, θ_N

2.3 Radius to Maximum Winds and Central Pressure Deficit

Figure 6 presents the cumulative probability distribution of radius to maximum winds for landfalling and exiting hurricanes and Figure 7 presents that for alongshore hurricanes.

The cumulative probability distributions of central pressure deficit for landfalling/alongshore and exiting hurricanes are presented in Figures 8 and 9, respectively.

Examination of historical hurricane data has demonstrated that the distributions for radius to maximum winds and central pressure deficit are not completely independent. The trend is such that the hurricanes with the more extreme central pressure deficit tend to be smaller. Figure 10 presents the ranges for R and Δp for the 300 n.mi. coast comprising the area of interest. This relationship of R and Δp is incorporated into the simulations to generate hurricanes in accordance with historical trend. For purposes of computer application, the joint cumulative probability distribution of R is modified to conform to the limited range shown on Figure 10 for any specific Δp selected within the range of -0.98 to -2.5 in. Hg.

2.4 Forward Speed

The cumulative probability distribution of the forward speed of translation for landfalling, alongshore and exiting hurricanes are presented in Figure 11.

2.5 Track Position

For the landfalling (or exiting) hurricanes, the track position is determined by y coordinate, Y_F, representing the landfall point as defined in Figure 3. Figure 12 presents the cumulative distribution for the actual landfalling position, Y_F, for landfalling and exiting hurricanes. Figure 13 presents the

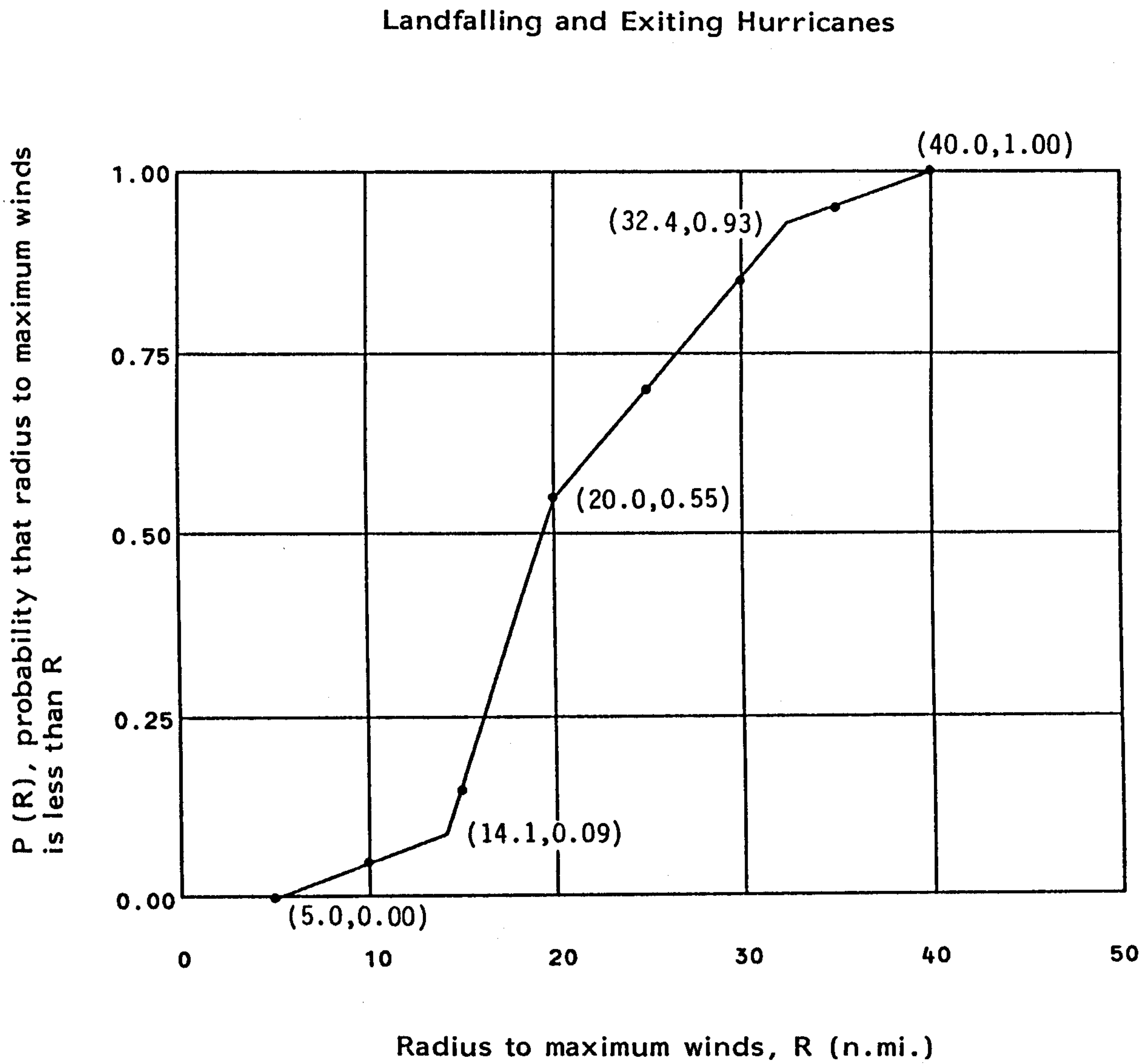

Figure 6 Cumulative Probability Distribution of Radius to Maximum Winds for Landfalling and Exiting Hurricanes

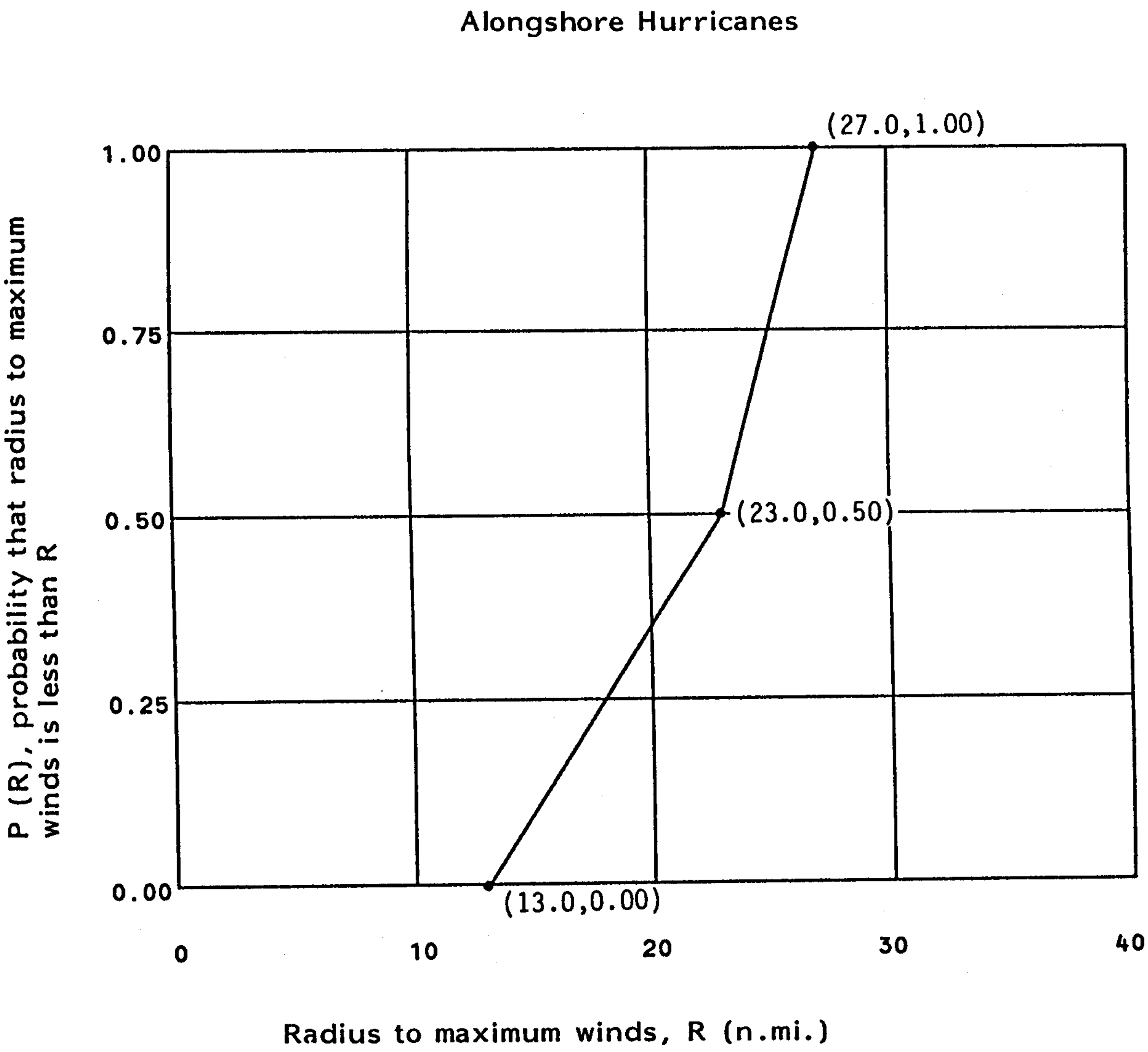

Figure 7 Cumulative Probability Distribution of Radius to Maximum Winds for Alongshore Hurricanes

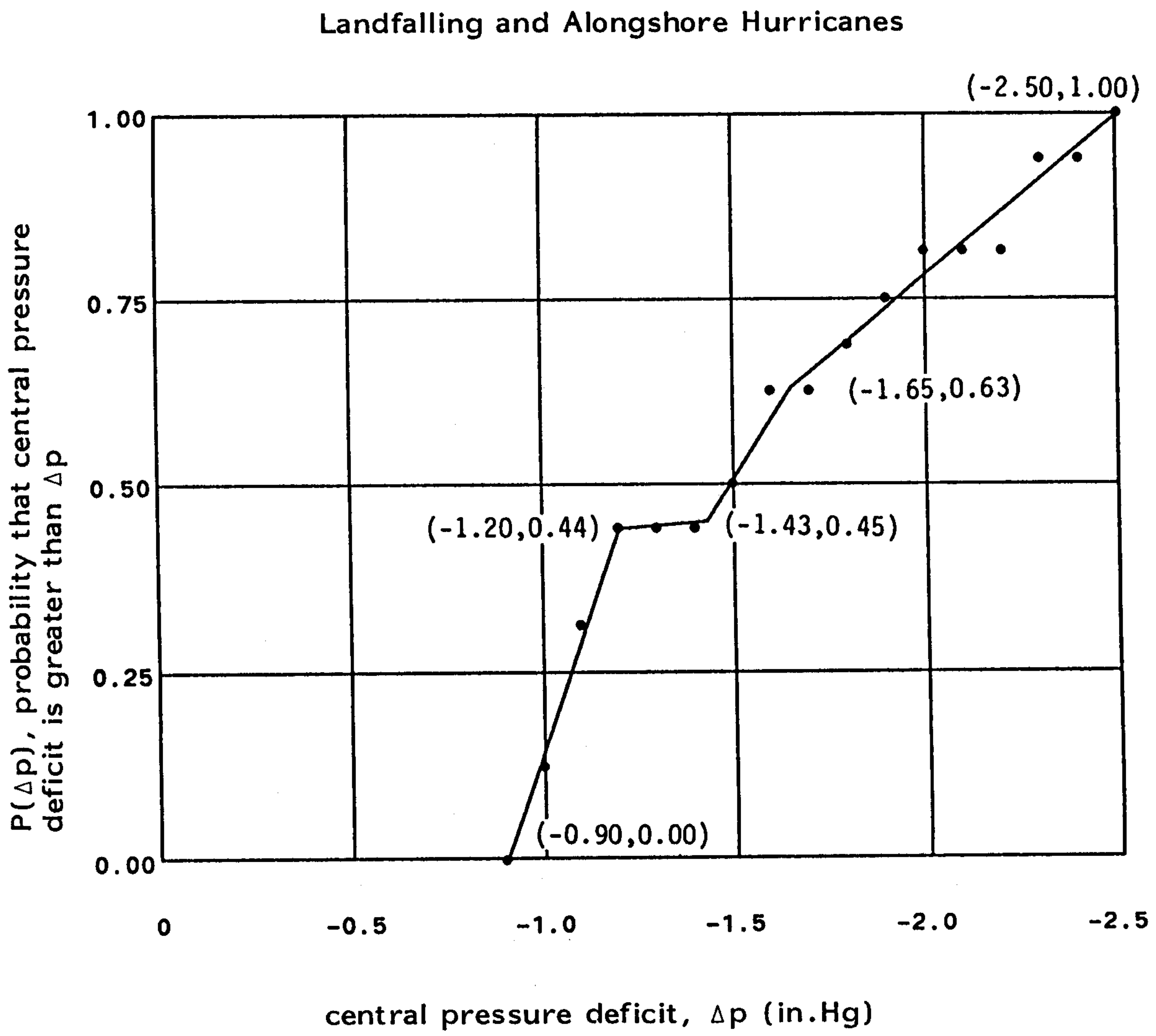

Figure 8 Cumulative Probability Distribution of Central Pressure Deficit, Δp, for Landfalling and Alongshore Hurricanes

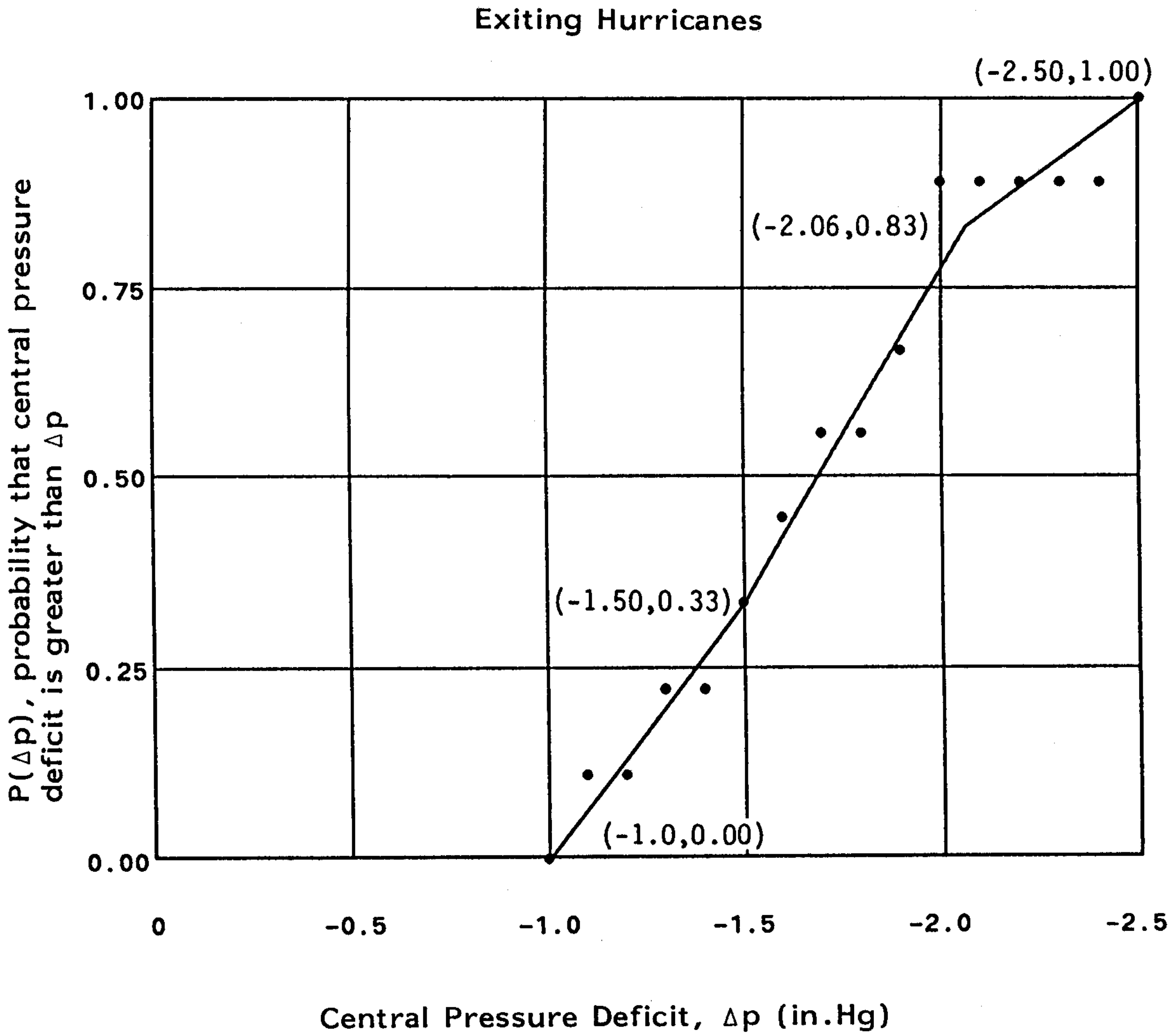

Figure 9 Cumulative Probability Distribution of Central Pressure Deficit, Δp, for Exiting Hurricanes

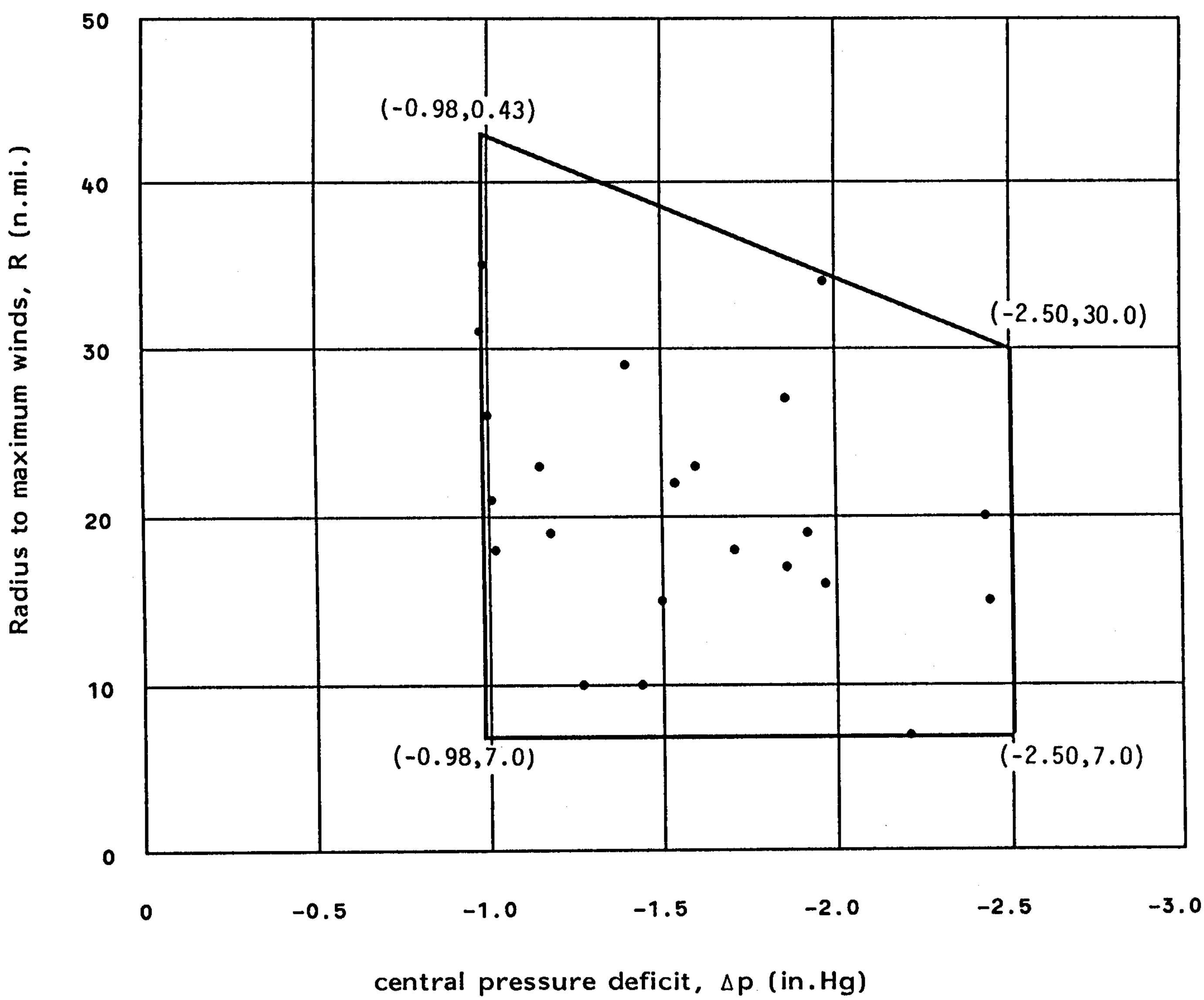

Figure 10 Historical Trend of Central Pressure Deficit, Δp, and Radius to Maximum Winds, R

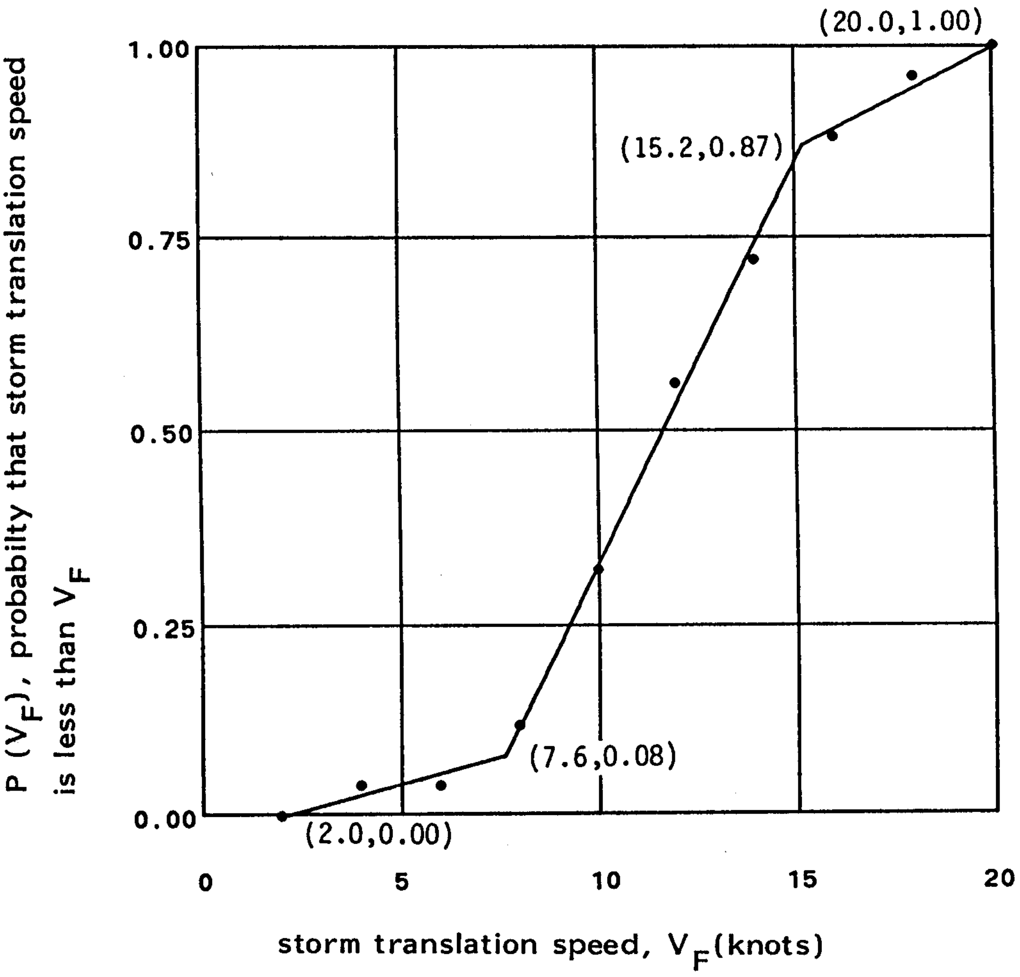

Figure 11 Cumulative Probability Distribution of Hurricane Translation Speed, V_F, for Landfalling, Alongshore and Exiting Hurricanes

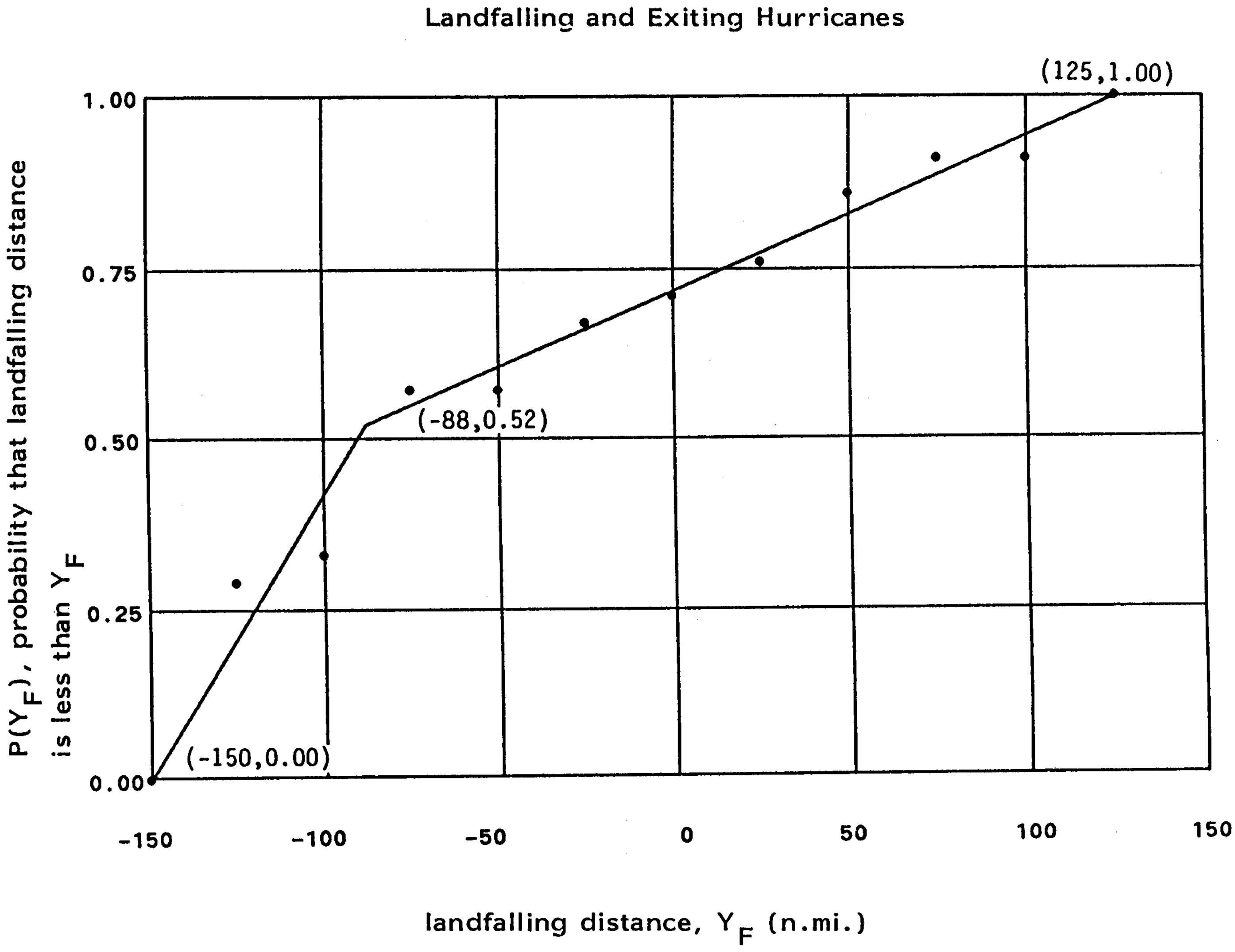

Figure 12 Cumulative Probability Distribution of Landfalling and Exiting Distance, Y_F, for Landfalling and Exiting Hurricanes

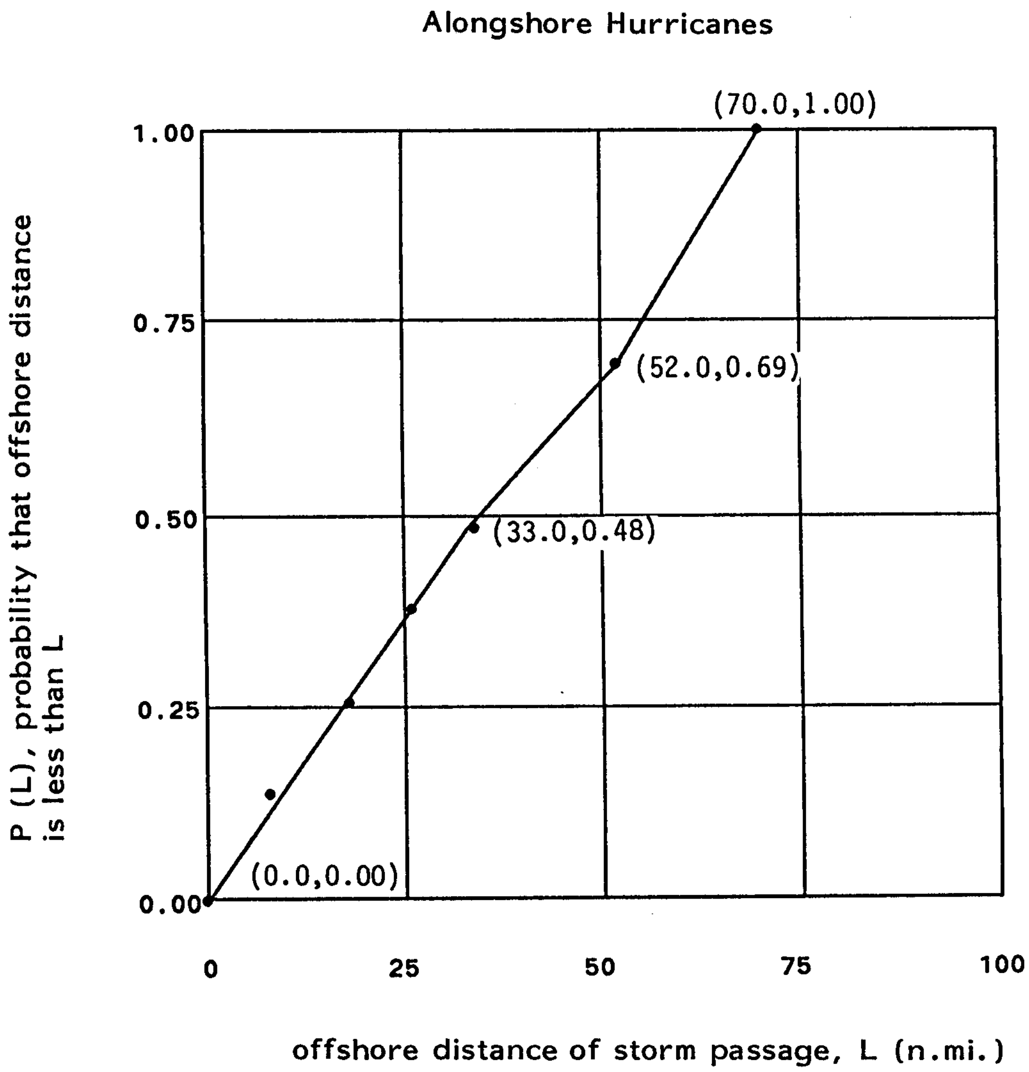

Figure 13 Cumulative Probability Distribution of Offshore Distance Passage, L, for Alongshore Hurricanes

cumulative distribution of offshore distance of passage, L, for alongshore hurricanes.

III. METHODOLOGY

3.1 Introduction

This section describes the overall methodology at a very general level to provide the reader with an understanding of the general procedures without addressing the details. The objective of this study is to develop, verify and apply procedures which will yield valid estimates of the combined total storm tides associated with various return periods at the site of interest.

The approach used here is to combine the available historical statistics of hurricanes with a set of numerical models to simulate the storm tides at the site of interest. Figure 14 is a flow chart illustrating the overall procedure. The numerical models include two-dimensional representations, with a variable grid version for the offshore and coastal areas. Prior to its application, the model is verified using tide gage measurements during hurricanes of 1947 and 1966. The two-dimensional model is significantly more expensive to operate and, because the simulation phase (which generates the statistics of the combined total storm tides) requires the computation of a few hundred hurricane events, a simpler, far less expensive one-dimensional model is developed and calibrated to yield reasonably good agreement with the predictions of the two-dimensional model. The following sections describe each of the elements in the overall calculation procedure.

3.2 Model Hurricane

The numerical models require, as input, some representation of the atmospheric pressures and winds which are responsible for the storm tide generation. For this purpose, a model hurricane is used that is characterized by the following five parameters:

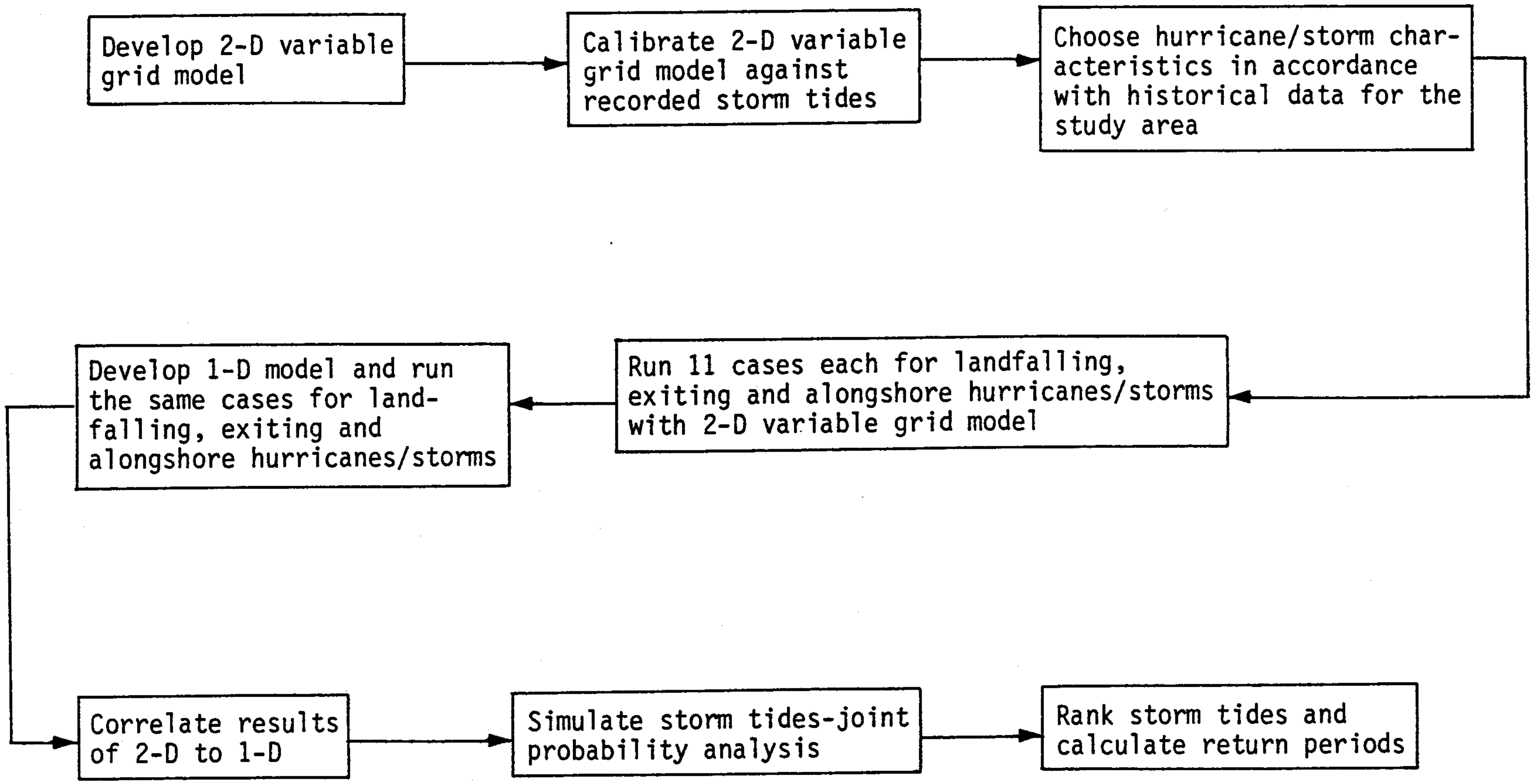

Figure 14 Flow Chart of Methodology

Δp = Central Pressure Deficit

R = Radius to Maximum Winds

V_F = Speed of Hurricane System Translation

θ = Hurricane Direction

Y_F = Landfall location or some other descriptor of hurricane track.

The model hurricane is one proposed by Wilson (5) and is characterized by circular isobars. The associated wind field is determined from a solution of the governing equations of motion. The model hurricane is described in Appendix B.

3.3 Features of the Two-Dimensional Numerical Model

As noted previously, there is a variable grid two-dimensional model for the offshore and coastal areas that affects the generation of storm tide for Sarasota County. The grids of the model are arranged in such a way that

1) The finest grids cover the coastal areas of Sarasota County to yield detailed information for the study. Fine grids are also used in locations where calibration of the model results against measured storm tides is to take place.

2) The coarsest grids cover the areas where detailed information is not needed.

3) A number of grids varying gradually in size are used for the transition from the coarsest to the finest grids and vice versa.

This arrangement of the varying grid system for the two-dimensional model gives good efficiency of computer time utilization.

The size of the finest grid is 1,000 ft. X 5,000 ft. and the coarsest 60,000 ft. X 42,750 ft. The two-dimensional model covers an area of 188.5 n.mi. X 201.7 n.mi. with the eastern side in approximate orientation with the shoreline of Sarasota County. Figure 15 shows the grid system layout.

The two-dimensional storm surge model is an implicit finite difference sys-

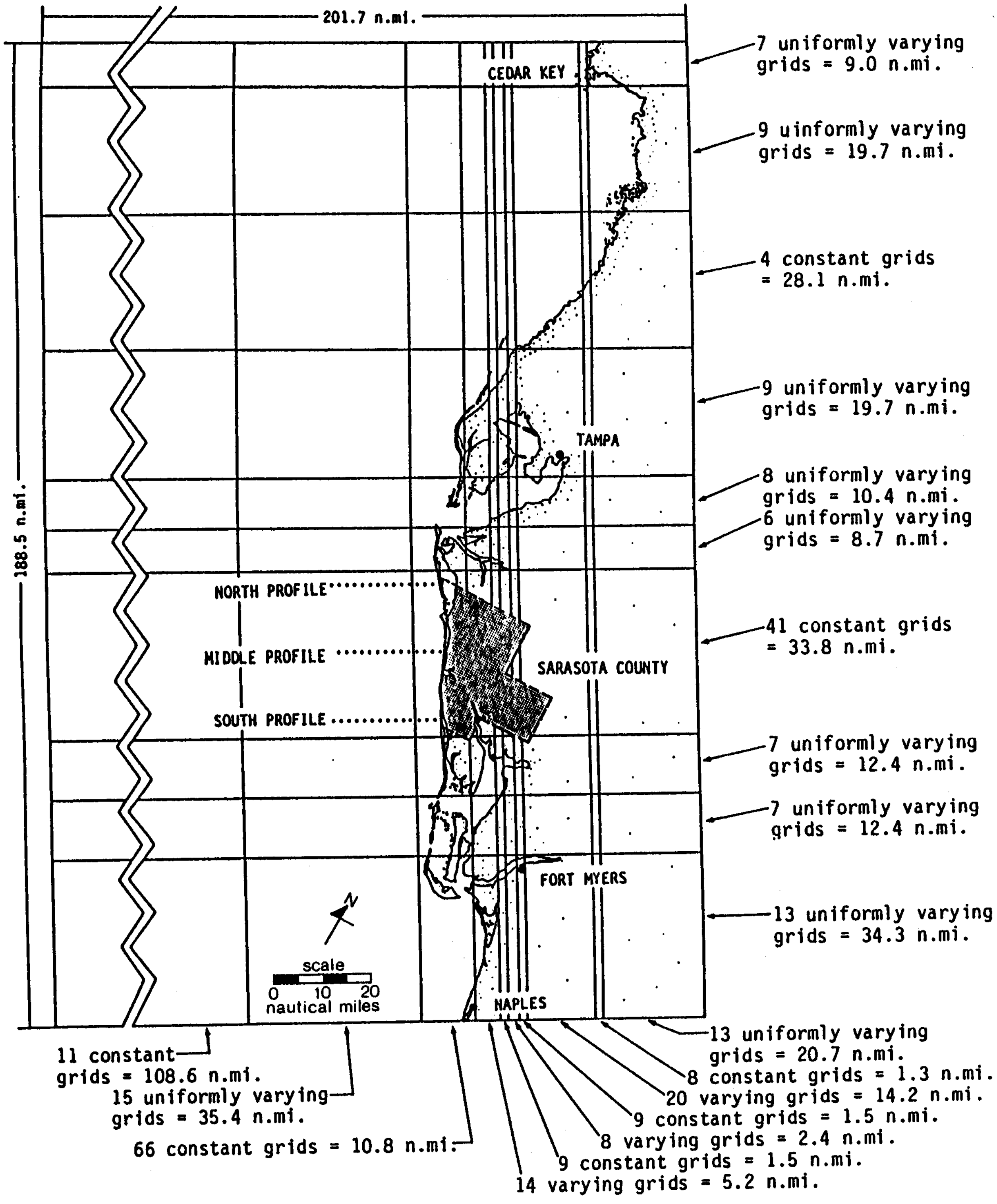

Figure 15 Grid System Layout for Sarasota County

tem in which the three governing differential equations are the two vertically averaged equations of momentum and the equation of continuity. The solution to the equations is carried out in a fractional time step procedure. The advantage of this fractional time step procedure is that it is time and space centered to the first order. The finite difference equations appropriate for implicit solution are solved by the "double sweep" method, which is described in detail in Chapter IV. The surface (wind) and bottom (friction) shear stresses, the barometric pressure, the Coriolis effect, the components of slope of the water surface and the boundary conditions are all incorporated into the solution processes.

Inlets and barrier islands which are too small to be resolved by the normal grid sizes are represented in the model by a special treatment. The boundary conditions specified on the two-dimensional model are that the water surface displacement on the boundaries where water is present are equal to the barometric head, due to atmospheric pressure variations. The normal discharge at these boundaries is that necessary to satisfy the volume requirement by the rising and falling water surface encompassed by the boundaries. Although this is an approximation, if the boundaries are sufficiently distant from the site of interest, any extraneous effects of this approximation should be small. The second type of boundary condition is the no-flow requirement which ensures that the flows are zero normal to grid lines where land elevations exist that are higher than the adjacent water elevations. At times when the elevation of a rising water surface exceeds the land elevation of an adjacent grid block, that block is flooded by a simple algorithm and vice versa for the "deflooding" from grid blocks at times that the falling water surface leaves a block exposed. The effects of vegetation on bottom and surface friction factors are accounted for in an approximate manner.

3.4 Features of the One-Dimensional Numerical Model

As noted earlier, a simple one-dimensional numerical model was developed and calibrated to allow the statistics to be generated based on simulation (calculations) of many hurricanes and associated storm tides.

The one-dimensional numerical model is described as follows. A transect line is established along a line which is approximately perpendicular to the bottom contours. The characteristics (Δp, R, θ_N, V_F and track) of the hurricanes are defined and the hurricane is advanced along the track line. The water surface displacement (boundary condition) at the seaward end of the transect line is taken as the static response of the water surface to the barometric pressure deviation at that point. The locations of the three transect lines (profiles) for Sarasota County are shown in Figure 15. Figures 16a, 16b and 16c present the profiles of the three transect lines and their one-dimensional grid representations.

3.5 Application of Numerical Models

The numerical models are applied in the following different phases:

1) Verifications of the two-dimensional numerical model against tide gage records of the September 1947 and June 1966 hurricanes.
2) Based on the characteristics of historical hurricanes, the two-dimensional model is run for 11 cases of landfalling, alongshore and exiting hurricanes with characteristics representative of the more probable and significant hurricanes.
3) The one-dimensional model is run for the same 11 cases for each type of hurricane described in 2) above. The storm tides developed in 2) then serve as a basis for adjusting the output of the one-dimensional model during the simulation phase.

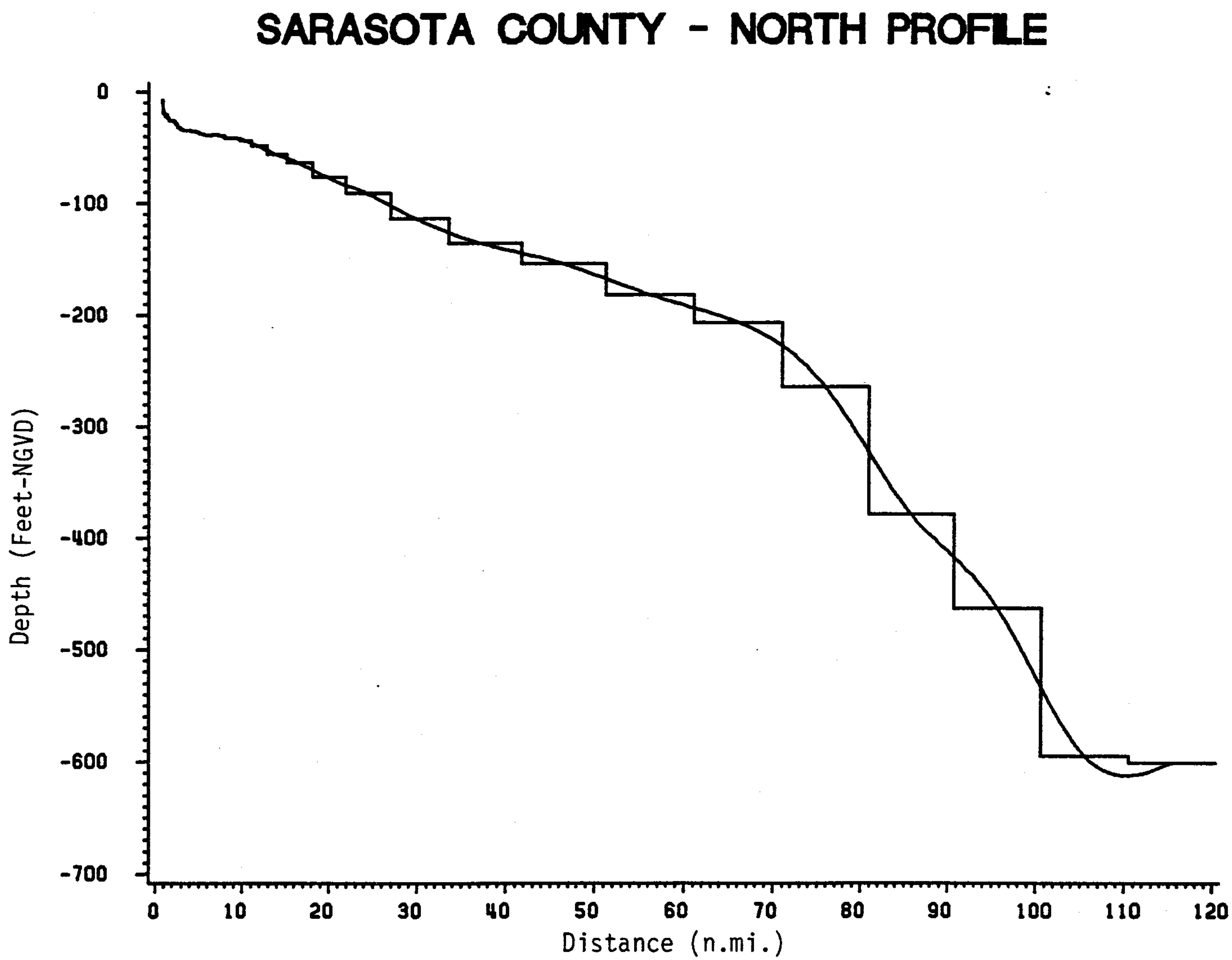

Figure 16a Profile of the North Transect Line and its One-Dimensional Grid Representation

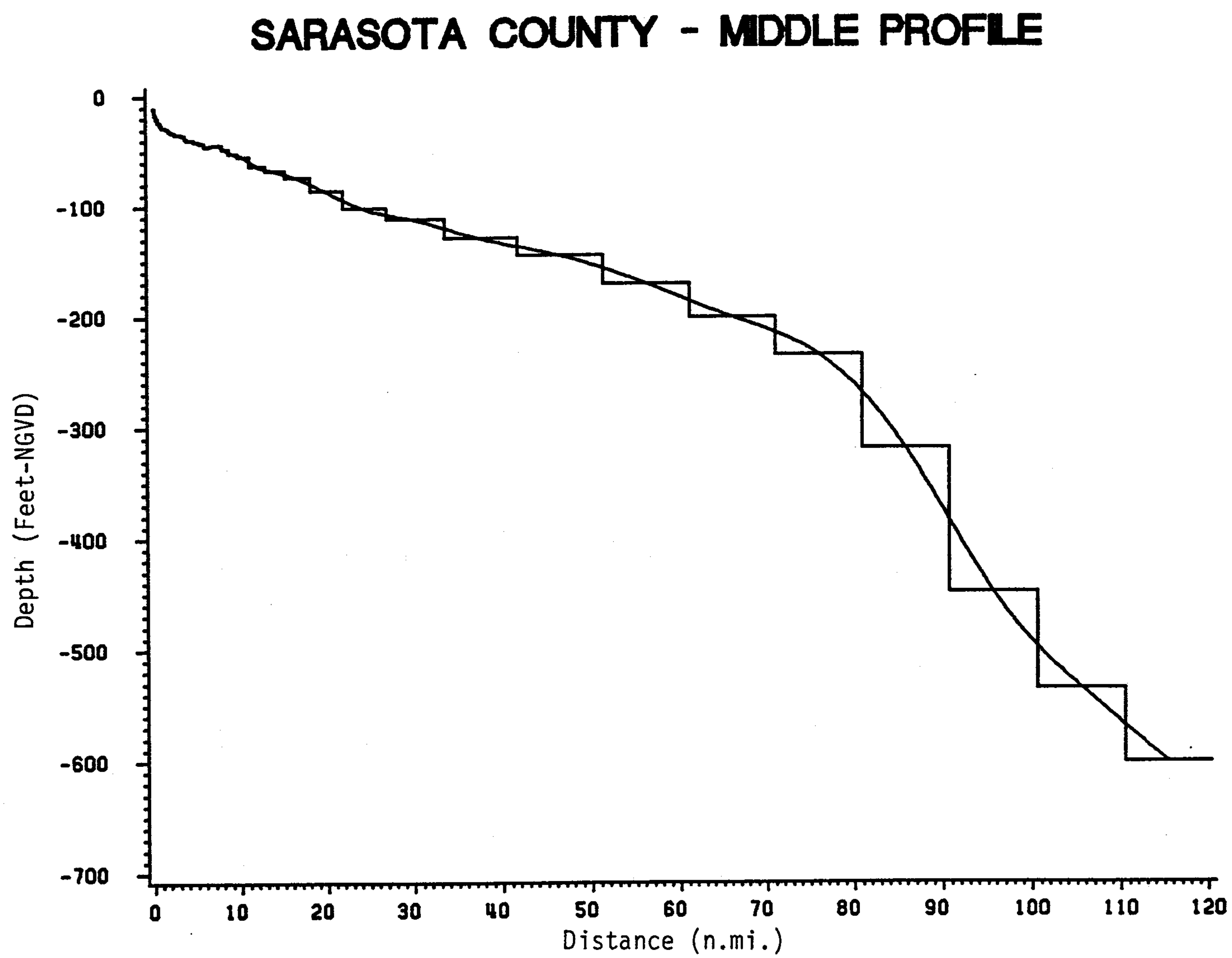

Figure 16b Profile of the Middle Transect Line and its One-Dimensional Grid Representation

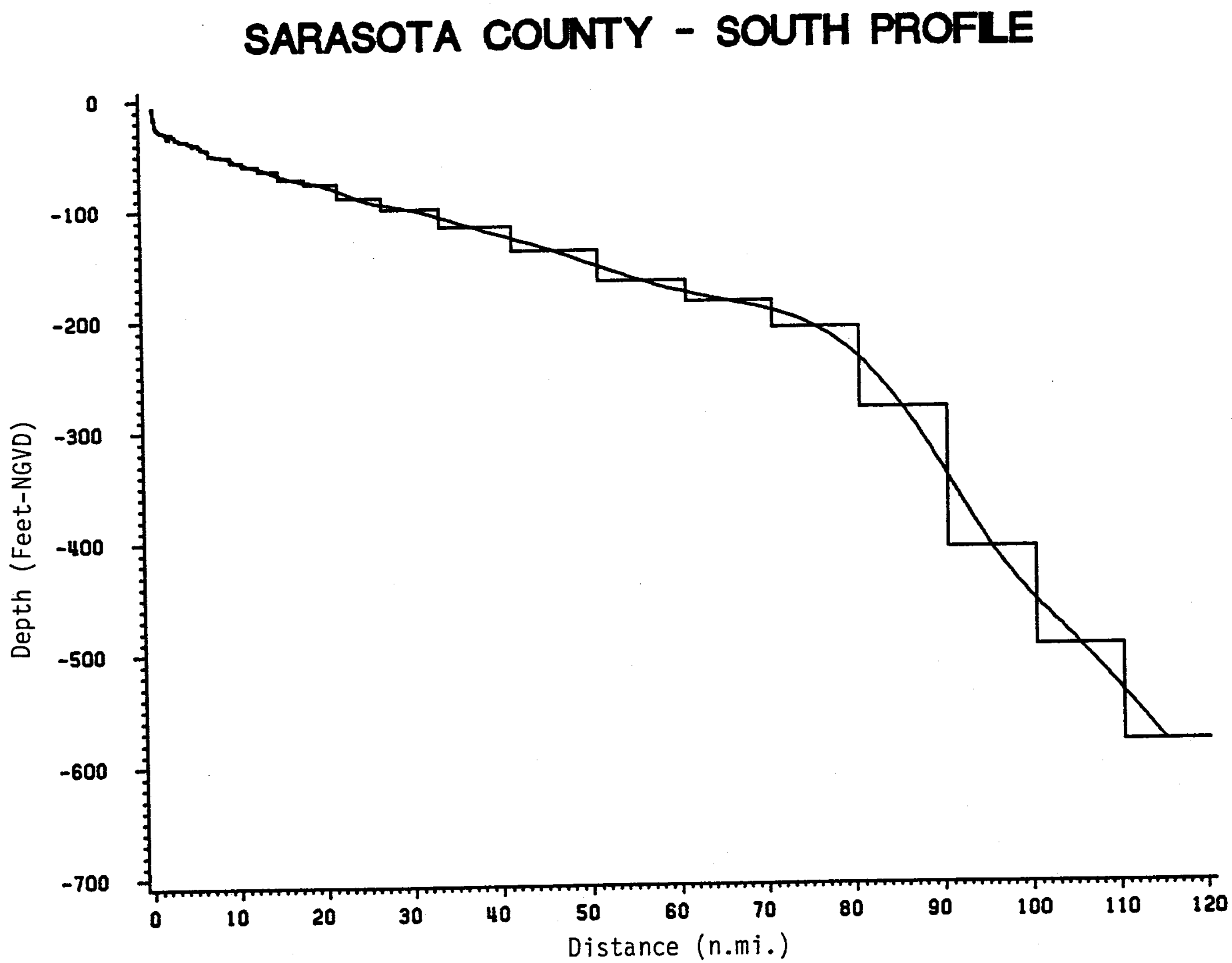

Figure 16c Profile of the South Transect Line and its One-Dimensional Grid Representation

3.6 Simulation of a n-Year Sequence of Hurricane Associated Storm Tides

With the statistical characteristics of historical hurricanes available and the simple one-dimensional model calibrated as described in the preceding section, the simulation shown in Figure 17 was carried out. The first phase of the simulation comprises the selection of the hurricane characteristics in accordance with the historical data. In each hurricane, this involves the following:

1) Quantifying Δp, R, V_F, θ and hurricane track in accordance with the historical probabilities.
2) For these characteristics, a random astronomical tide from the hurricane season is generated as a boundary condition to the one-dimensional numerical model and the model is run to determine the storm surge at the site of interest. This storm surge with dynamic wave set-up is then adjusted in accordance with the factors obtained from the two-dimensional model calibration runs for the landward grid at each time step to yield the combined total storm tide.
3) Determining whether enough hurricanes have been simulated for the n-year simulation.
4) After the required number of hurricanes and associated storm tides have been simulated, the peak water levels for each hurricane are ranked and the return period, TR, is calculated, according to

$$TR = 2000/M$$

where M is the rank of the combined total storm tide level. (For example, if the simulation was carried out for a 2,000 year period, the highest combined total tide level would have a return period of 2,000 years, the fourth highest water level would have a return period of

3.6 Simulation of a n-Year Sequence of Hurricane Associated Storm Tides

With the statistical characteristics of historical hurricanes available and the simple one-dimensional model calibrated as described in the preceding section, the simulation shown in Figure 17 was carried out. The first phase of the simulation comprises the selection of the hurricane characteristics in accordance with the historical data. In each hurricane, this involves the following:

1) Quantifying Δp, R, V_F, θ and hurricane track in accordance with the historical probabilities.
2) For these characteristics, a random astronomical tide from the hurricane season is generated as a boundary condition to the one-dimensional numerical model and the model is run to determine the storm surge at the site of interest. This storm surge with dynamic wave set-up is then adjusted in accordance with the factors obtained from the two-dimensional model calibration runs for the landward grid at each time step to yield the combined total storm tide.
3) Determining whether enough hurricanes have been simulated for the n-year simulation.
4) After the required number of hurricanes and associated storm tides have been simulated, the peak water levels for each hurricane are ranked and the return period, TR, is calculated, according to

$$TR = 2000/M$$

where M is the rank of the combined total storm tide level. (For example, if the simulation was carried out for a 2,000 year period, the highest combined total tide level would have a return period of 2,000 years, the fourth highest water level would have a return period of

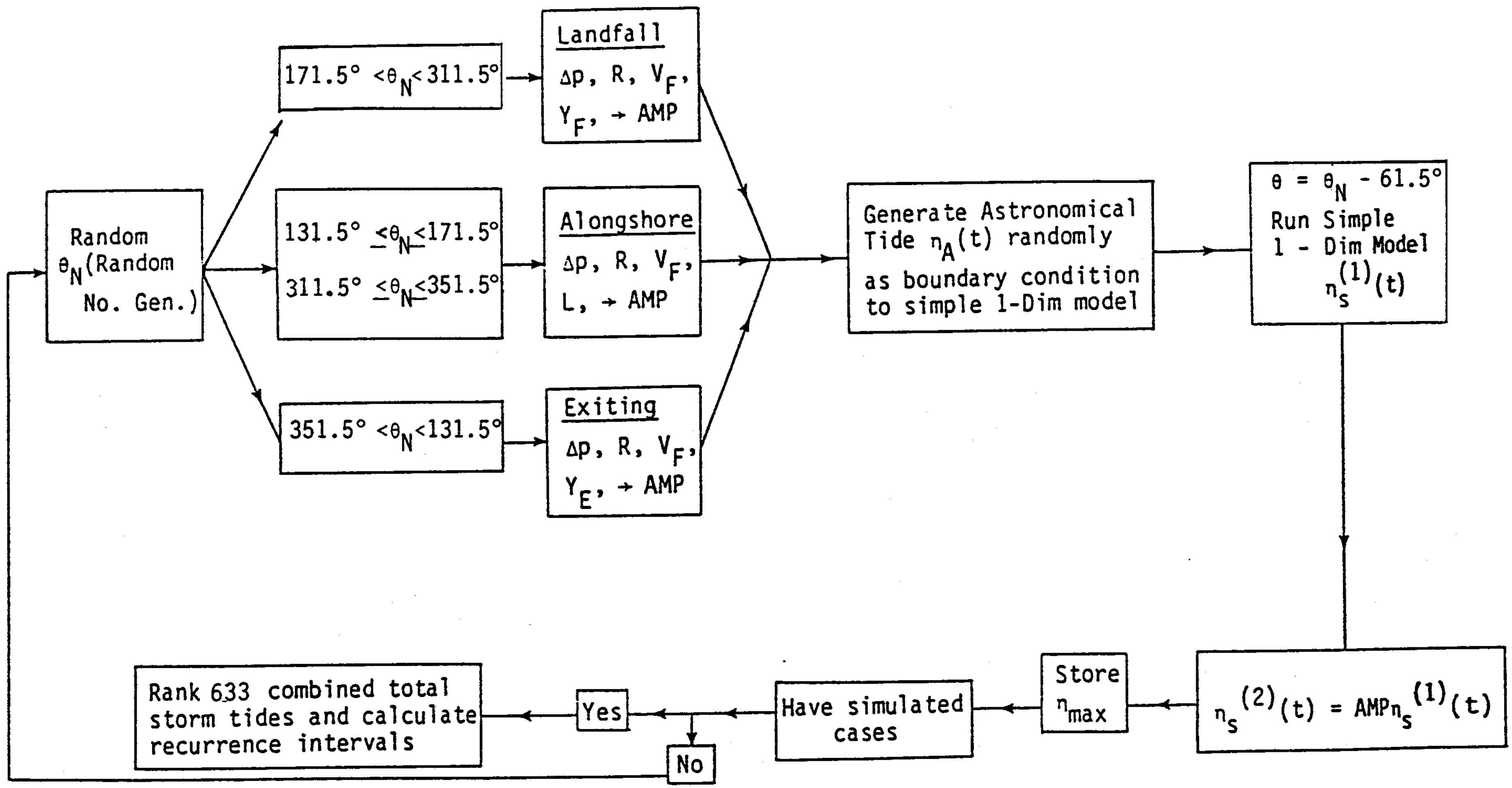

Figure 17 Flow Chart for Storm Tide Simulations (After Calibration to Determine AMP)

500 years, etc.). Finally, by presenting these results on semi-log paper, it is possible to interpolate the return periods of interest, i.e., TR = 10, 50, 100, 200 and 500 years, to yield the final results for the present study.

IV. NUMERICAL MODELS-DESCRIPTION AND CALIBRATION

As noted in the previous chapter the methodology included the development, calibration and application of a series of numerical models and statistical hurricane characteristics to the simulation of a long period (2,000 years) to establish storm water levels associated with various return periods of interest. Figure 14 presents a flow chart of the methodology. This chapter parallels that of Chapter III; however, much greater detail is presented. The following subsections review the various numerical models and calibration of calculation procedures.

4.1 Two-Dimensional Numerical Model

Variable-Grid Two-Dimensional Numerical Model - The grid associated with this numerical model relative to the shoreline is presented in Figure 15. The coarsest grid of the model is 9.87 n.mi. x 7.04 n.mi. and the finest is 0.16 n.mi. x 0.82 n.mi. and the purpose of the numerical model is to calculate the storm tides as the storm translate across the shelf.

Governing Differential Equations - The governing differential equations for the two-differential model are the two vertically averaged equations of momentum and the equation of continuity, given by:

Momentum Equations

$$\frac{\partial q_x}{\partial t} + \frac{q_x}{D}\frac{\partial q_x}{\partial x} + \frac{q_y}{D}\frac{\partial q_x}{\partial y} = -gD\frac{\partial \eta}{\partial x} - \frac{D}{\rho}\frac{\partial p}{\partial x} + \frac{\tau_{w_x}}{\rho} - \frac{\tau_{b_x}}{\rho} - \beta q_y \quad (1)$$

$$\frac{\partial q_y}{\partial t} + \frac{q_x}{D}\frac{\partial q_y}{\partial x} + \frac{q_y}{D}\frac{\partial q_y}{\partial y} = -gD\frac{\partial \eta}{\partial y} - \frac{D}{\rho}\frac{\partial p}{\partial y} + \frac{\tau_{w_y}}{\rho} - \frac{\tau_{b_y}}{\rho} + \beta q_x \quad (2)$$

Continuity Equation

$$\frac{\partial \eta}{\partial t} + \frac{\partial q_x}{\partial x} + \frac{\partial q_y}{\partial y} = 0 \quad (3)$$

in which

$\begin{Bmatrix} q_x \\ q_y \end{Bmatrix}$ = volumetric transport components per unit width in the $\begin{Bmatrix} x \\ y \end{Bmatrix}$ directions

t = time

D = total water depth $(h+\eta)$ including the still water depth, h and the storm surge, η

η = storm surge above mean water level

x = horizontal coordinate, directed offshore

y = horizontal coordinate direction according to the left-hand coordinate system

g = gravitational constant

ρ = mass density of water

p = barometric pressure

$\begin{Bmatrix} \tau_{w_x} \\ \tau_{w_y} \end{Bmatrix}$ = wind shear stress components in the $\begin{Bmatrix} x \\ y \end{Bmatrix}$ directions

$\begin{Bmatrix} \tau_{b_x} \\ \tau_{b_y} \end{Bmatrix}$ = bottom shear stress components in the $\begin{Bmatrix} x \\ y \end{Bmatrix}$ directions

f = Darcy-Weisbach friction coefficient

β = Coriolis parameter = $2\Omega \sin \psi$

Ω = angular speed of earth rotation = 7.27×10^{-5} rad/sec

ψ = latitude of site of interest

The surface and bottom shear stress components are related to the wind speed W and discharge components by:

$$\begin{Bmatrix} \tau_{w_x} \\ \tau_{w_y} \end{Bmatrix} = \rho K W \begin{Bmatrix} W_x \\ W_y \end{Bmatrix} \tag{4}$$

$$\begin{Bmatrix} \tau_{b_x} \\ \tau_{b_y} \end{Bmatrix} = \frac{\rho f |q|}{8D^2} \begin{Bmatrix} q_x \\ q_y \end{Bmatrix} \qquad |q| = \sqrt{q_x^2 + q_y^2} \tag{5}$$

in which K is an air-sea friction coefficient developed by Van Dorn (6); and and depends on the wind speed as follows:

$$K = \begin{cases} 1.1 \times 10^{-6} & \text{for } W < W_{cr} \\ 1.1 \times 10^{-6} + 2.5 \times 10^{-6} \left(1 - \frac{W_{cr}}{W}\right)^2 & \text{for } W \geq W_{cr} \end{cases} \tag{6}$$

where W_{cr} = 23.6 ft/sec.

The quantity, f, is the Darcy-Weisbach bottom friction coefficient and varies with depth, bottom roughness and vegetation, if present. For purposes of this study, f was developed by Christensen and Walton (7) of the University of Florida and is presented in Figure 18.

Finite Difference Forms of Governing Differential Equations - The finite difference representations of Equations (1), (2) and (3) are expressed as follows with the convective terms (i.e. $\frac{q_x}{D}\frac{\partial q_x}{\partial x}$, etc.) omitted in preparation for an implicit type of solution. The solution to the equations will be carried out in a fractional time step procedure. This procedure is schematized in Figure 19. The advantage of this fractional time step procedure is that it is time and space centered to the first order.

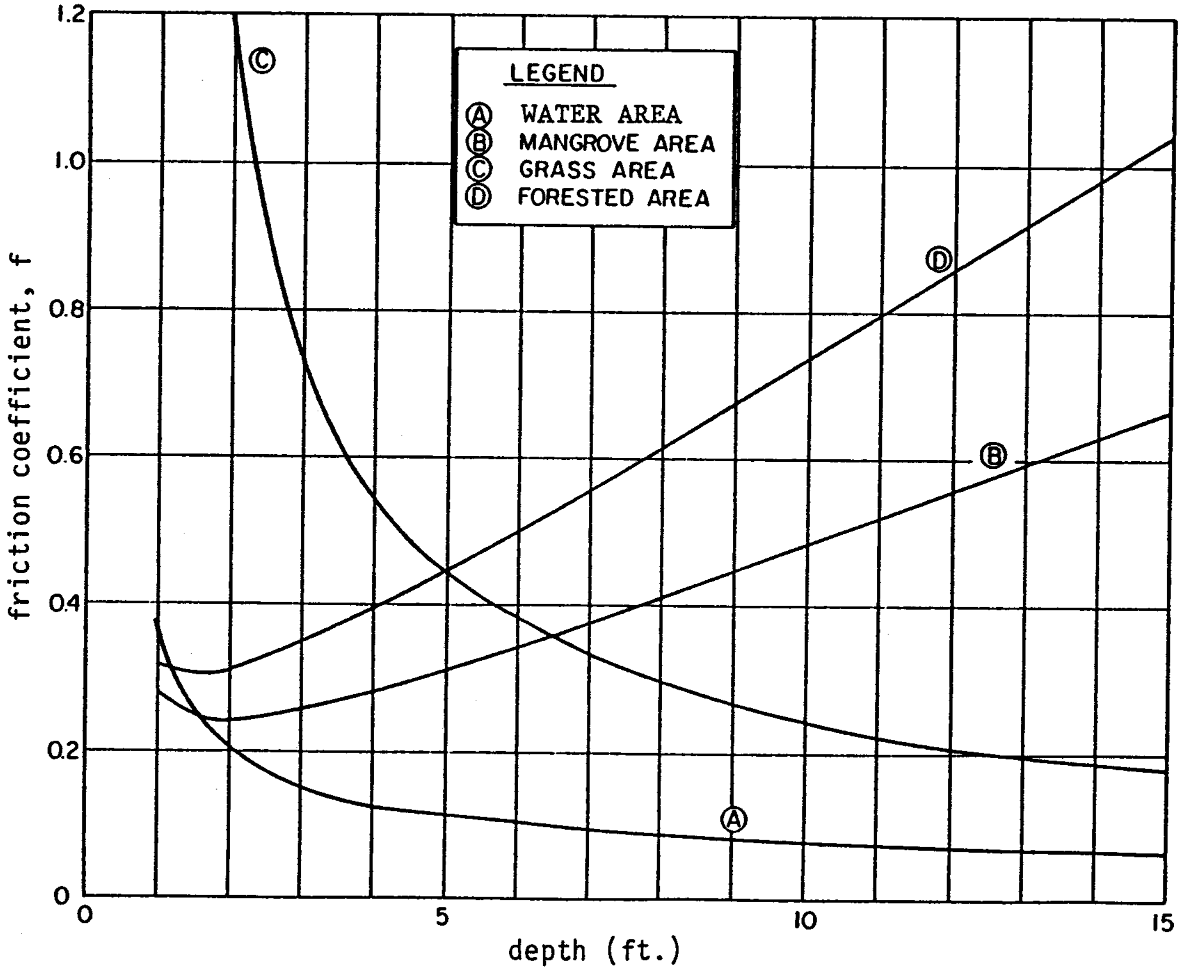

Figure 18 Bottom Friction Coefficients of Various Bottom Conditions

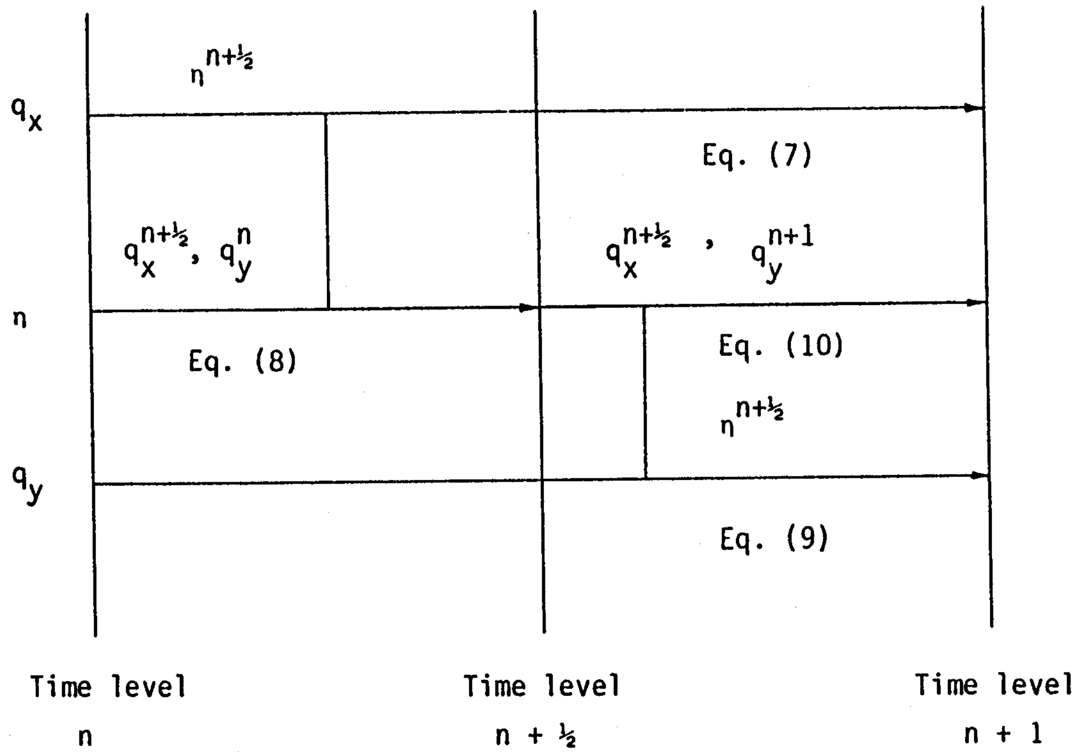

Notes: (1) Vertical links denote equations which are solved simultanteously.

(2) Values adjacent to the horizontal bars indicate the time level of the different variables entering into the computations.

Figure 19 Schematic of Implicit Method of Solving Momentum and Continuity Equations

The finite difference equations for the first portion of the fractional time step that are appropriate for the implicit method of solution are:

$$A_i \, \eta_{i,j}^{n+\frac{1}{2}} + B_i \, q_{x_{i,j}}^{n+1} + C_i \, \eta_{i-1,j}^{n+\frac{1}{2}} = D_i \tag{7}$$

$$A_i^* \, q_{x_{i+1,j}}^{n+1} + B_i^* \, \eta_{i,j}^{n+\frac{1}{2}} + C_i^* \, q_{x_{i,j}}^{n+1} = D_i^* \tag{8}$$

where Eq. (7) represents the momentum equation in the x-direction and Eq. (8) represents the continuity equation; these two equations are to be solved simultaneously. The second set of simultaneous equations which is solved subsequent to the solution of the first set is:

$$A_j \, \eta_{i,j}^{n+\frac{1}{2}} + B_j \, q_{y_{i,j}}^{n+1} + C_j \, \eta_{i,j-1}^{n+1} = D_j \tag{9}$$

$$A_j^* \, q_{y_{i,j+1}}^{n+1} + B_j^* \, \eta_{i,j}^{n+1} + C_j^* \, q_{y_{i,j}}^{n+1} = D_j^* \tag{10}$$

Implicit Solution of the Finite Difference Equations - The solution for each time step progresses by first solving Eqs. (7) and (8) simultaneously for each j grid line sweeping over all values of i. This establishes the values of $\eta^{n+\frac{1}{2}}$ and q_x^{n+1} for the entire (i,j) field. The procedure is then repeated for Eqs. (9) and (10) in which this pair of equations is solved simutaneously for η^{n+1} and q_y^{n+1} for the entire (i,j) field. This latter pair of equations is expressed sequentially for each value of i, then solved for all values of j, for that particular i grid line. The expressions for the various coefficients are presented as follows.

$$A_i = g(\overline{h+\eta}) \frac{\Delta t}{\Delta x}$$

$$B_i = 1 + \frac{f|q_{i,j}^{n}|\Delta t}{8(\overline{h+\eta})^2}$$

$$C_i = -A_i$$

$$D_i = q^n_{x_{i,j}} + \Delta t \left[\frac{(\overline{h+\eta})}{\rho} \frac{\partial p}{\partial x} + \frac{\tau_{w_{x_{i,j}}}}{\rho} - \beta(\overline{q_y})^n \right]$$

$$A^*_i = \frac{\Delta t}{4\Delta x}$$

$$B^*_i = 1.0$$

$$C^*_i = -\frac{\Delta t}{4\Delta x}$$

$$D^*_i = \eta^n_{i,j} - \frac{1}{4}\frac{\Delta t}{\Delta x} \left(q^n_{x_{i+1}} - q^n_{x_i} \right) - \frac{\Delta t}{2\Delta y} \left(q^n_{y_{i,j+1}} - q^n_{y_{i,j}} \right)$$

$$\overline{q}^{\,n}_{y_{i,j}} = \frac{1}{4} \left[q^n_{y_{i-1,j}} + q^n_{y_{i,j}} + q^n_{y_{i-1,j+1}} + q^n_{y_{i,j+1}} \right]$$

$$\left| q^n_{y_{i,j}} \right| = \sqrt{\left(q^n_{x_{i,j}} \right)^2 + \left(\overline{q}^{\,n}_{y_{i,j}} \right)^2}$$

$$A_j = \frac{g(\overline{h+\eta})}{2} \frac{\Delta t}{\Delta x}$$

$$B_j = 1 + \frac{f|q^n_{i,j}|\Delta t}{8(\overline{h+\eta})^2}$$

$$C_j = -A_j$$

$$D_j = q^n_{y_{i,j}} + \Delta t \left[-\frac{g(\overline{h+\eta})}{2\Delta x} \Delta t \left(\eta^n_{i,j} - \eta^n_{i,j-1} \right) - \frac{(\overline{h+\eta})}{\rho} \frac{\partial p}{\partial y} \right.$$

$$\left. + \frac{\tau_{w_{y_{i,j}}}}{\rho} + \beta(\overline{q_x})^n \right]$$

$$\overline{q}^{\,n}_{x_{i,j}} = \frac{1}{4} \quad q^n_{x_{i,j}} + q^n_{x_{i,j-1}} + q^n_{x_{i+1,j}} + q^n_{x_{i+1,j-1}}$$

$$\left| q^n_{x_{i,j}} \right| = \sqrt{\left(\overline{q}^{\,n}_{x_{i,j}} \right)^2 + \left(q^n_{y_{i,j}} \right)^2}$$

$$A^*_j = \frac{\Delta t}{2\Delta y}$$

$$B^*_j = 1.0$$

$$C^*_j = -A^*_j$$

$$D^*_j = \eta^{n+\frac{1}{2}}_{i,j} - \frac{\Delta t}{4\Delta x}\left(q^n_{x_{i+1,j}} - q^n_{x_{i,j}} \right) - \frac{\Delta t}{4\Delta x}\left(q^{n+1}_{x_{i+1,j}} - q^{n+1}_{x_{i,j}} \right)$$

With the coefficients now specified, the method of solving the sets of simultaneous equations will be described. The method is termed the "double sweep" method in which the first sweep involves "conditioning" two sets of auxiliary coefficients (E_i, F_i, E^*_i, F^*_i). The second sweep determines the values of η and q and, in the process, incorporates the required boundary conditions. The procedure will be illustrated for Equations (7) and (8) and it is noted that the same exact procedure is applicable to solving Equations (9) and (10). The procedure commences by establishing two auxiliary equations with four variables (E_i, F_i, E^*_i, F^*_i) which are initially unknown,

$$\eta^{n+\frac{1}{2}}_{i,j} = E_i \, q^{n+1}_{x_{i,j}} + F_i \tag{11}$$

$$q^{n+1}_{x_{i+1,j}} = E^*_i \, \eta^{n+\frac{1}{2}}_{i,j} + F^*_i \tag{12}$$

Eqs. (11) and (12) are substituted in Eqs. (7) and (8) and the results simplified to yield

$$q^{n+1}_{x_{i,j}} = -\frac{C_i}{A_iE_i+B_i} \, \eta^{n+\frac{1}{2}}_{i-1,j} + \frac{D_i-A_iF_i}{A_iE_i+B_i} \tag{13}$$

$$\eta^{n+\frac{1}{2}}_{i,j} = -\frac{C^*_i}{A^*_iE^*_i+B^*_i} \, q^{n+1}_{x_{i,j}} + \frac{D^*_i-A^*_iF^*_i}{A^*_iE^*_i+B^*_i} \tag{14}$$

Comparison of Eqs. (13) and (14) establishes the values of the unknown coefficients (E,F,E*,F*) in terms of the known coefficients (A,B,...,A*,B*,...).

The expressions are

$$E_i = -\frac{C_i^*}{A_i^* E_i^* + B_i^*}, \quad F_i = \frac{D_i^* - A_i^* F_i^*}{A_i^* E_i^* + B_i^*} \tag{15}$$

$$E_{i-1}^* = -\frac{C_i}{A_i E_i + B_i}, \quad F_{i-1}^* = \frac{D_i - A_i F_i}{A_i E_i + B_i} \tag{16}$$

To illustrate the manner in which boundary condition information is incorporated into the procedure, suppose that water surface level, η, is specified at i = IMAX and that q_x is specified as zero at i = 2[§]. The first sweep commences by noting (from Eq. 11) that

$$E_i^* = F_i^* = 0.0 \tag{17}$$

With the values of E_{IMAX} and F_{IMAX} not known, E_{IMAX-1}^* and F_{IMAX-1}^* can be calculated from Eqs. (16), then values of E_{IMAX-1} and F_{IMAX-1} computed from Eqs. (15) and so on. E_i^* and F_i^* are set equal to

$$E_{IMAX} = 0.0$$
$$F_{IMAX} = \eta_{IMAX,j}^{n+\frac{1}{2}} \tag{18}$$

in accordance with the boundary condition and Eq. (12). This completes the first sweep and establishes all the coefficients over the grid line.

The second sweep simply consists of applying the methodology to the y-direction as described in detail for the x-direction. In summary, the "double sweep" procedure as presented here progresses from large i to small i for the

---

§ It is noted that other combinations of boundary conditions at the two ends of the grid line could be accomodated. Also, internal boundary conditions of the type $q_{x_{i,j}}^{n+1} = 0$ are satisfied by the choice of coefficients: $E_{i-1}^* = F_{i-1}^* = 0$.

first sweep and then progresses back from small i to large i for the second sweep.

It can be shown that this procedure results in an exact solution of the tridiagonal set of simultaneous equations represented by Eqs. (7) and (8). As noted previously the same procedure is then applied to solve Eqs. (9) and (10) which completes establishing η, q_x and q_y at the $(n+1)^{th}$ time step.

4.2 Boundary Conditions

To complete formulation of the problem, boundary conditions must be specified at the boundaries of the grid presented in Figure 15. On the "open" (water) boundaries, the water surface is specified to be that associated with the barometric pressure, i.e.

$$\eta_{B_{i,j}} = \left(\frac{p_\infty - p_{i,j}}{\rho g}\right) \qquad (19)$$

in which p_∞ denotes the far field barometric pressure. In addition, on the open boundary grid cells, it is specified that only discharge components perpendicular to the boundaries occur and that these discharges on the exterior boundaries of the grid system are those required to satisfy the continuity equation (Eq. 8).

On the "closed" boundaries, i.e., at the shoreline where land elevations are higher than the adjacent water elevations, a no-flow boundary condition is specified perpendicular to that boundary. However, "flooding" and "deflooding" of grid blocks adjacent to the boundaries can occur. Flooding occurs when the water level is greater by a specified small amount than the ground elevation of an adjacent grid block. When this condition exists, the grid block is activated by a simple allocation of this excess elevation on the newly activated block and in subsequent time steps the grid block is incorporated into the normal calculation scheme. Deflooding occurs when the water level on a grid block drops below a specified level leaving a very small depth on that block. The block is "deactivated" and the excess water placed on the adjacent grid.

The solution is started from an initial condition of zero water surface displacement and zero discharge components. The hurricane system is translated along a specified path at a designated speed. At each time step, the hurricane effects (represented by the pressure and wind stress components) on each cell are calculated and the finite-difference equations (Eq. 7, 8, 9, and 10) employed. The results are updated values of η, q_x and q_y for each cell.

4.3 One-Dimensional Numerical Model

The one-dimensional numerical model is significantly less expensive and simpler to run and is used in the simulation phase, in order to generate the required data within budgetary constraints. The justification for using the one-dimensional model is that it can be adequately calibrated with the rather complete two-dimensional model.

The one-dimensional numerical model is a static model and therefore no effects of inertia are included. The finite difference forms of the governing one-dimensional differential equations are:

$$\eta_{i+1}^{n+1} = \eta_i^{n+1} + \frac{\Delta x}{g(\overline{h+\eta})} \left[\frac{\tau_{w_{x_i}}}{\rho} - \beta\, q_{y_i}^{n+1}\right] + \frac{p_i^{n+1} - p_{i+1}^{n+1}}{\rho g} \qquad (20)$$

$$q_{y_i}^{n+1} = \frac{1}{BB} \left[q_{y_i}^{n} + \frac{\Delta t}{\rho}\, \tau_{w_{y_i}}\right] \qquad (21)$$

where $BB = 1.0 + \frac{f \cdot \Delta t \left|q_{y_i}^n\right|}{(\overline{h+\eta})^2}$ and the remaining variables are as defined previously for the two-dimensional model.

The one-dimensional model is initiated from a condition of rest ($q_y = 0$) and zero water surface displacement ($\eta = 0$). The only boundary condition required is that at the seaward end ($i = 1$) of each transect where the "barometric tide" is imposed as

$$\eta_1 = \frac{p_\infty - p_1}{\rho g} \qquad (22)$$

In applying the one-dimensional numerical model, a variable grid size (1,000 ft. to 60,000 ft.) is used as presented in Figures 16a, 16b and 16c.

4.4 Simulation

To summarize information presented earlier, this phase includes the simulation of the occurrence of 2,000 years of hurricanes along a shoreline segment of 300 n.mi. The simulated hurricanes include landfalling, alongshore and exiting hurricanes with directional distributions according to Figure 5. In an average 2,000 year period, there would be a total of 633 hurricanes.

Selection of Hurricane Parameters - Each of the five idealized hurricane parameters [Radius to Maximum Winds, R; Central Pressure, p_0 (or Central Pressure Deficit, Δp); Track Direction, θ_N; System Forward Speed, V_F; and Track Position] is determined randomly in accordance with the associated cumulative probability distribution functions. The procedure is described below for the track direction, θ_N, and is similar for all other variables.

The approximate piece-wise linear cumulative probability distribution function for track direction, θ_N, is shown in Figure 5. The nature of this function is such that the more predominant directions are those where the function rises steeply. To randomly select a track direction in accordance with the distribution function, the computer first generates a random number between 0 and 1 corresponding to the cumulative probability. Suppose that this number is 0.60. Since this value corresponds to the linear segment between directions of 180.0° and 230.0°, the computer interpolates to find a track direction, θ_N, of 198.42°.

We note that this is a landfalling hurricane. The other four parameters are determined similarly with a separate and independent random number being generated for each parameter and the appropriate cumulative probability distribution used.

Calculation of Storm Surge with the Effect of Astronomical Tide - A particular hurricane can be "phased" such that the maximum resulting storm surge is increased or decreased by astronomical tidal fluctuations. Considering the predicted astronomical tidal fluctuations at Captiva Island from June 1 to November 30, 1984 to be representative of those occurring during the hurricane season and assuming the phasing of hurricane occurrence and astronomical tides to be independent, the combination of these tidal components was carried out in the following manner.

With the hurricane parameters established, a starting time for the hurricane is selected randomly between June 1 and November 30, 1984. The corresponding astronomical tide at the starting time is generated as the boundary condition in the one-dimensional model and varies with time thereafter according to the input astronomical tide data. The calculation of the storm surge history by the calibrated one-dimensional model is thus phased with the astronomical tide to yield the combined storm surge and astronomical tide water level history at the site of interest.

Dynamic Wave Set-Up - When waves break, a shoreward directed force in addition to the wind stress, is exerted on the water in the surf zone. This causes an additional rise in water level termed "wave set-up". This effect has been studied extensively in the laboratory [Saville (8), Bowen et al. (9)] and tide gage measurements during severe storms have confirmed its importance in nature. Most of the information relative to wave set-up has been developed for "regular" waves, that is for a wave train in which each wave is the same as the preceding wave. Waves in nature, however, are not regular and tend to occur in groups. A recent analytic study by Lo (10) has shown that for natural wave trains there is a dynamic wave set-up that is approximately 50% larger than would be predicted by a static treatment. In order to evaluate this result, model studies were conducted in the large University of Florida wave tank. It was found that the experimental and analytical results by Lo were in approximate agreement.

The maximum dynamic wave set-up, η'_{max}, across the surf zone can be shown to be approximately

$$\eta'_{max} = 0.285 \left[1 - 2.82 \left(\frac{H_b}{gT^2}\right)^{\frac{1}{2}} \right] H_b \tag{23}$$

which includes the dynamic factor of 50% and in which T is the wave period and H_b is the breaking wave height based on the deep water significant wave height, H_o, taken approximately as

$$H_b = 0.94\ H_o \tag{24}$$

The deep water significant wave height is determined from an extension of a method recommended for hurricane generated waves as summarized in the Shore Protection Manual (11),

$$(H_o)_{max} = 16.5\ e^{R(\Delta p/100)} \left(1 + \frac{0.208\ V_F}{\sqrt{W_R}}\right) \tag{25}$$

where R = radius to maximum winds in nautical miles, Δp = central pressure deficit in inches of mercury, V_F = translation speed of hurricane in knots, and W_R = maximum sustained wind speed in knots. For purposes here, the local effective deep water significant wave height is based on the local winds, W, at the surf zone area of interest and the maximum winds in the hurricane, W_{max}, as

$$H_o = (H_o)_{max}(W/W_{max})^2 \qquad (26)$$

Equations 23, 24, 25 and 26 provide the basis for determining the maximum dynamic wave set-up within the surf zone. The computed value of η'_{max} was added to the nearshore storm surge. It is stressed that η'_{max} represents the maximum dynamic wave set-up across the surf zone and that this value varies with time (because the wind speed varies with time). The value of η'_{max} was computed at each time step for the shoreward grid, and added to the corresponding surge value resulting from wind stress, barometric pressure and the effect of astronomical tide to yield the combined total storm tide history.

With this combined total storm tide history thus determined, it is a simple matter to search in the computer to obtain the maximum of the combined total storm tide at the site of interest.

4.5 Computation of Return Periods

With a sufficient number (633) of maximum combined total storm tides simulated to represent a typical 2,000 year time interval, the tides associated with various return periods of interest are determined. The 633 maximum combined total storm tides were ranked in descending order with the largest occurring first. The return period, TR, of the ranked tides is then

$$TR = 2000/M \qquad (27)$$

in which

TR = Return period in years between expected exceedances of the associated maximum storm tide

M = Rank of maximum storm tide

As an example, for $M = 633$ (associated with the lowest water level) the return period would be:

$$TR_{633} = 2000/633 = 3.16 \text{ years}$$

which indicates that the smallest storm tide could be expected to be exceeded approximately once every 3.16 years. As a second example, the return period for $M = 4$ is

$$TR_4 = 2000/4 = 500 \text{ years}$$

The ranked maximum total storm tide and associated return periods can be plotted and the total storm tide associated with any return period determined.

Finally, it is noted that it is possible to run the simulation procedure any number of times to determine the stability (constancy) of any combined total storm tide associated with a given return period. It is expected that for a 2,000 year simulation, the storm tides associated with the longer (> 500 year) return periods would not be well-defined by one simulation and would exhibit variation from simulation to simulation. However, the storm tides associated with the lower return periods ($TR \leq 200$ years) should be well-defined by a 2,000 year simulation and hence are not expected to vary significantly for various simulations.

Table I

Input Parameters for Calibration Hurricanes

1. Hurricane of September 1947

date	time (EST)	Δp (in. Hg)	V_F (knots)	R (n. mi.)	θ_N (degrees)
9/18	1900	-1.95	5.34	34.0	90.0
9/19	0100	-1.95	6.54	34.0	107.8
	0700	-1.39	13.03	34.0	117.4
	1300	-1.39	17.90	34.0	116.6
	1900	-1.39	22.20	34.0	122.7
9/20	0100	-1.39	20.92	34.0	121.7
	0700	-1.39	12.24	34.0	109.1
	1300	-1.27	11.40	34.0	110.5

Starting Coordinates:

X_S = -30.35 n. mi.

Y_S = -89.53 n. mi.

Landfalling Coordinates:

X_F = -2.42 n. mi.

Y_F = -74.68 n. mi.

2. Hurricane Alma of June 1966

date	time (EST)	Δp (in. Hg)	V_F (knots)	R (n. mi.)	θ_N (degrees)
6/08	0700	-1.22	15.03	23.0	183.4
	1300	-1.27	15.11	23.0	173.2
	1900	-1.15	17.17	23.0	158.7
6/09	0100	-1.22	17.91	23.0	146.9
	0700	-1.27	9.17	23.0	168.8
	1300	-0.95	7.47	23.0	216.6
	1900	-1.07	12.03	23.0	234.4
6/10	0100	-1.07	12.03	23.0	234.4

Starting Coordinates:

X_S = 127.98 n. mi.

Y_S = -235.70 n. mi.

Landfalling Coordinates:

X_F = 37.14 n. mi.

Y_F = 4.44 n. mi.

Figures 20, 21 and 22 show the computed and measured storm tides at Cedar Key, Venice Inlet and Fort Myers, respectively. While the measured peak storm tide is 1.5 ft. higher than that computed at Cedar Key, the difference between the measured and computed peak storm tides is less than 0.4 ft. at the other two locations.

2. Hurricane Alma of June 1966

Tide gage recordings during this hurricane are available (NOAA). Figures 23, 24 and 25 show the measured and computed storm tides at Cedar Key, St. Petersburg and Fort Myers, respectively. While the measured peak storm tide is 0.7 ft. higher than that computed at Cedar Key, the measured and computed peak storm tide difference is within 0.4 ft. at the other two locations.

The consistent lower prediction of peak storm tides at Cedar Key, which has also happened in other calibrations/verifications, could be caused by local conditions or the remote location of the area in the two-dimensional model. Otherwise, it appears that the two-dimensional model yields reasonably good results in locations close to the study area. The calibration of the two-dimensional model is thus taken as 1.00, i.e. the calculated storm tides do not have to be adjusted.

5.3 Calibration of One-Dimensional Numerical Model

Eleven cases for each of the three types of hurricanes are run using the two-dimensional model to establish the peak surge at the site of interest. The characteristics of these hurricanes and the peak storm surges at the site are presented in Tables IIa and IIb for landfalling model hurricanes, IIIa and IIIb for alongshore model hurricanes and IVa and IVb for exiting model hurricanes.

A calibration relationship between the peak surges computed from the one-

V. CALIBRATION RATIONALE AND RESULTS

5.1 Rationale

Ideally there are sufficient storm tide data (from tide gages) at a site of interest to allow calibration of the numerical model. If this is the case, then it would be possible to calibrate the one-dimensional numerical model with data from the site and it would not be necessary to utilize the two-dimensional model described earlier. Unfortunately, there are not sufficient tide measurements at the site, and it is therefore necessary to utilize the two-dimensional model as an intermediate representation.

The calibration procedure followed is, first, to validate/calibrate the two-dimensional numerical model using tide gage data for hurricanes of 1947 and 1966. With this calibration as a basis for the two-dimensional model, it is then run for a series of hurricanes with parameters encompassing representative ranges. These include 11 cases each for landfalling, alongshore and exiting hurricanes to determine the peak storm tides at the site. These results are then utilized to calibrate the one-dimensional numerical model which is run for the same 11 cases for each of the three types of hurricanes.

5.2 Results--Calibration of Two-Dimensional Numerical Model

The calibration is conducted by running the two-dimensional model for the hurricane characteristics presented in Table I and the results are then compared with the measurements. The data used and the calibration results are as follows:

1. Hurricane of September 1947

   There are tide recordings at Cedar Key, Venice Inlet and Fort Myers within the area covered by the two-dimensional numerical model.

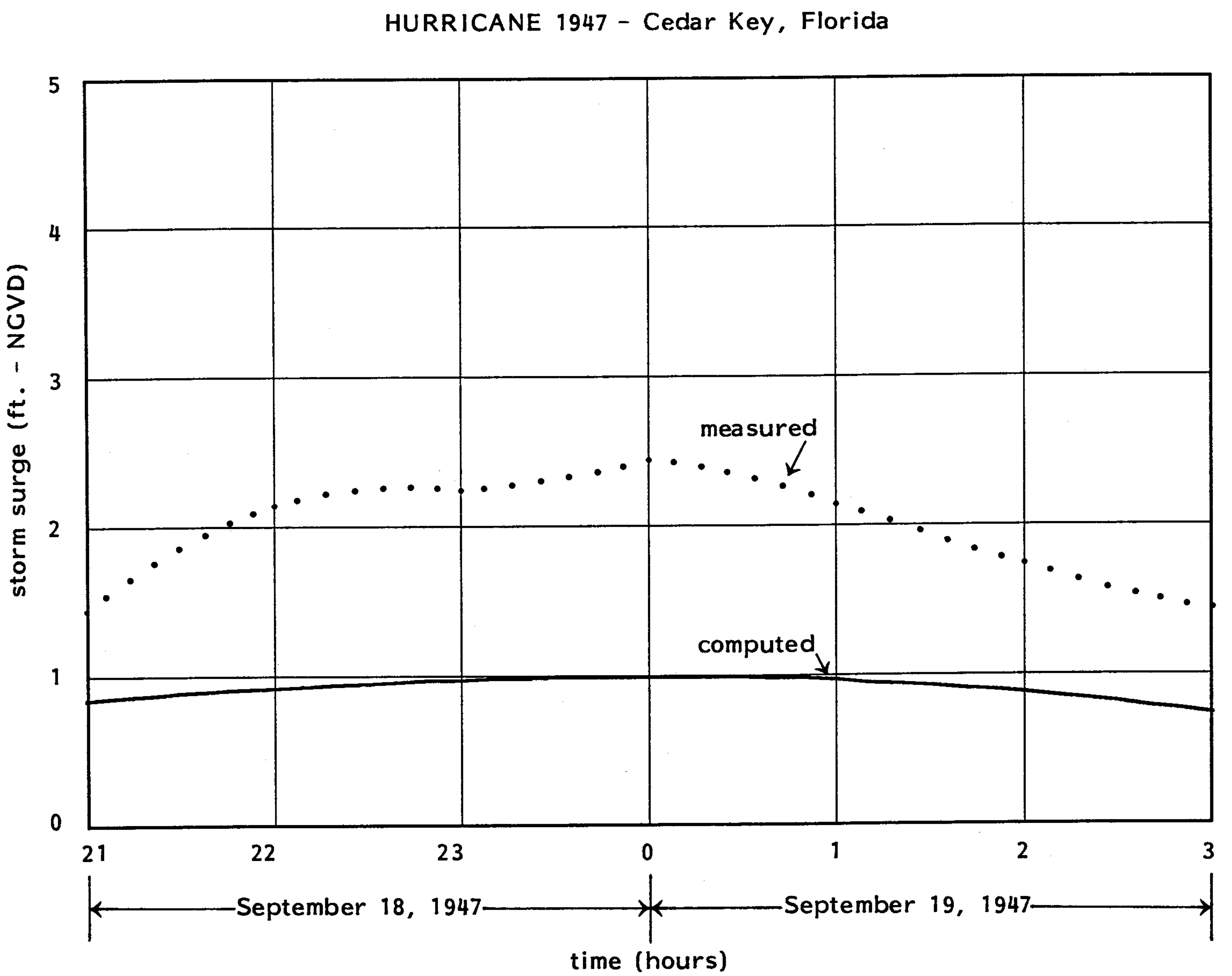

Figure 20 Comparison between Measured and Computed Storm Tide at Cedar Key, Florida for September 1947 Hurricane

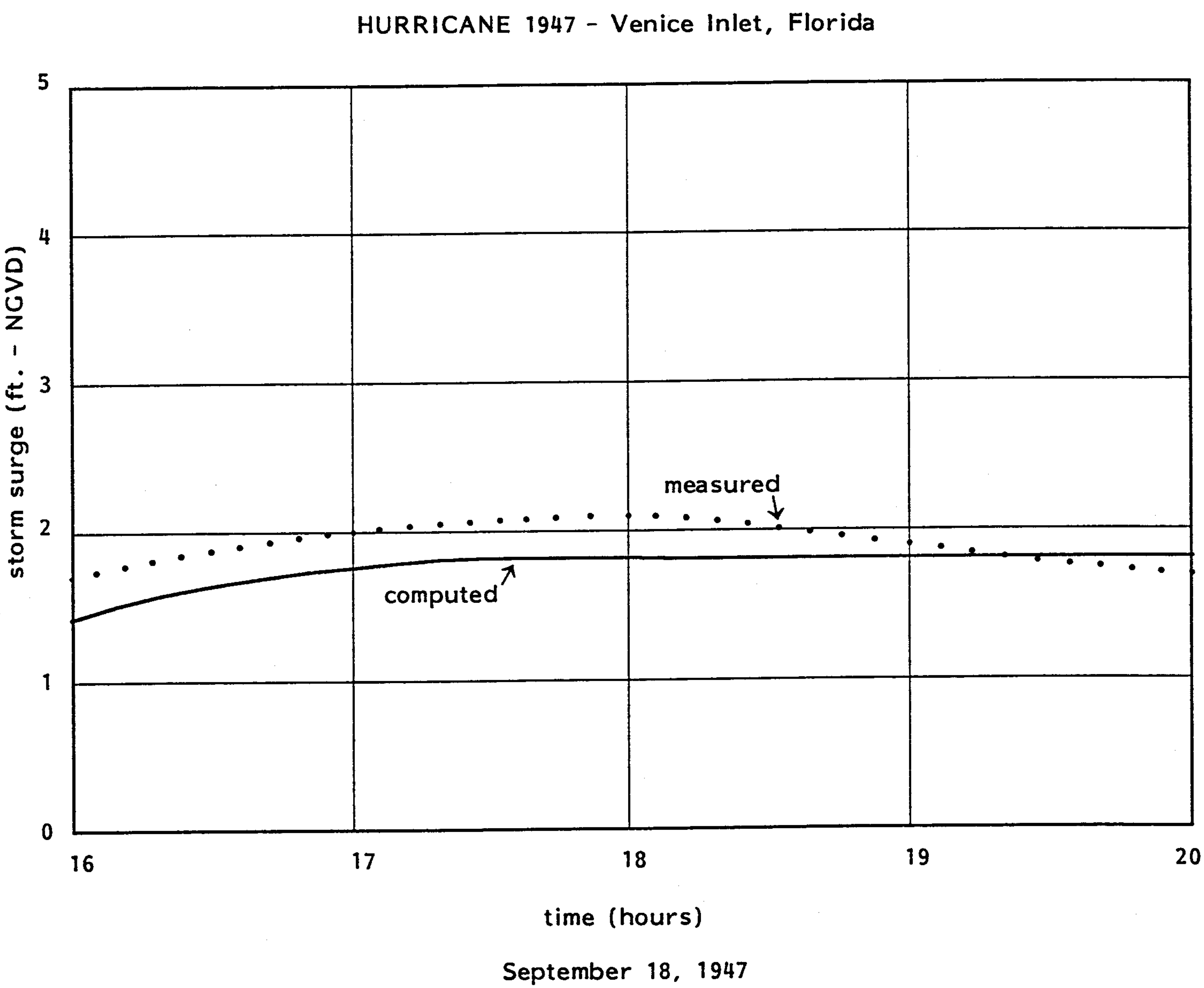

Figure 21 Comparison between Measured and Computed Storm Tide at Venice Inlet, Florida for September 1947 Hurricane

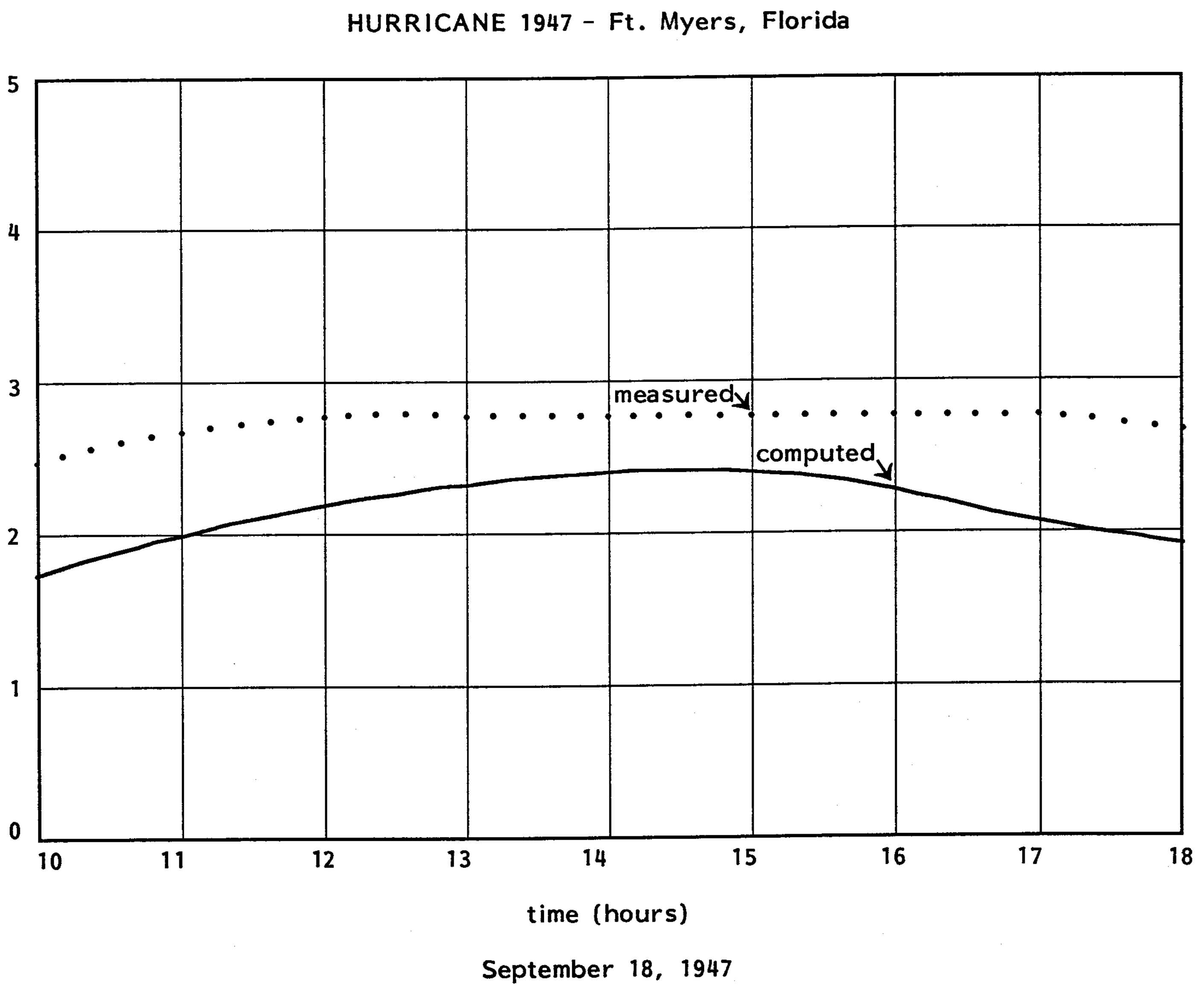

Figure 22 Comparison between Measured and Computed Storm Tide at Ft. Myers, Florida for September 1947 Hurricane

HURRICANE ALMA - Cedar Key, Florida

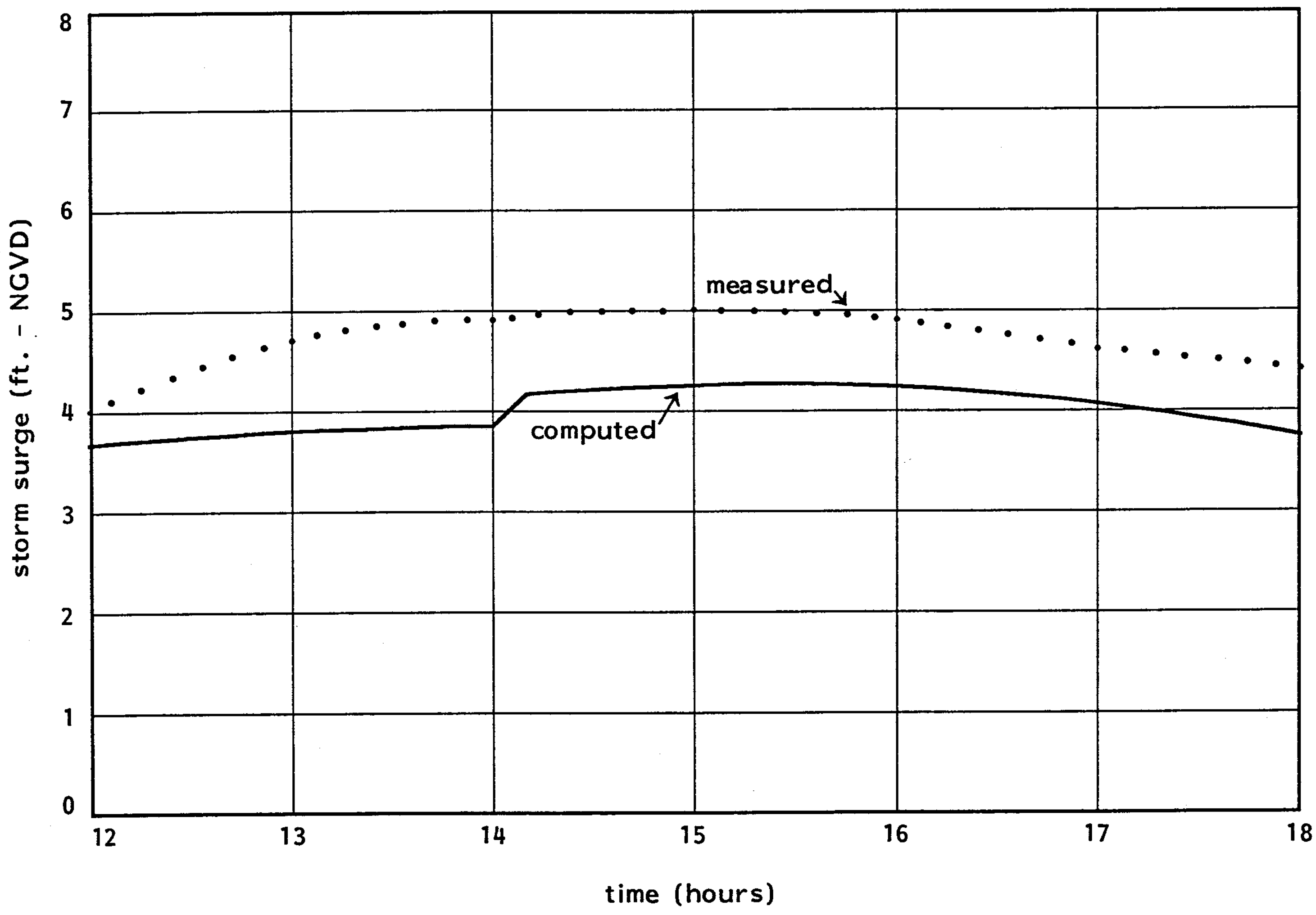

Figure 23 Comparison between Measured and Computed Storm Tide at Cedar Key, Florida for Hurricane Alma, June 1966

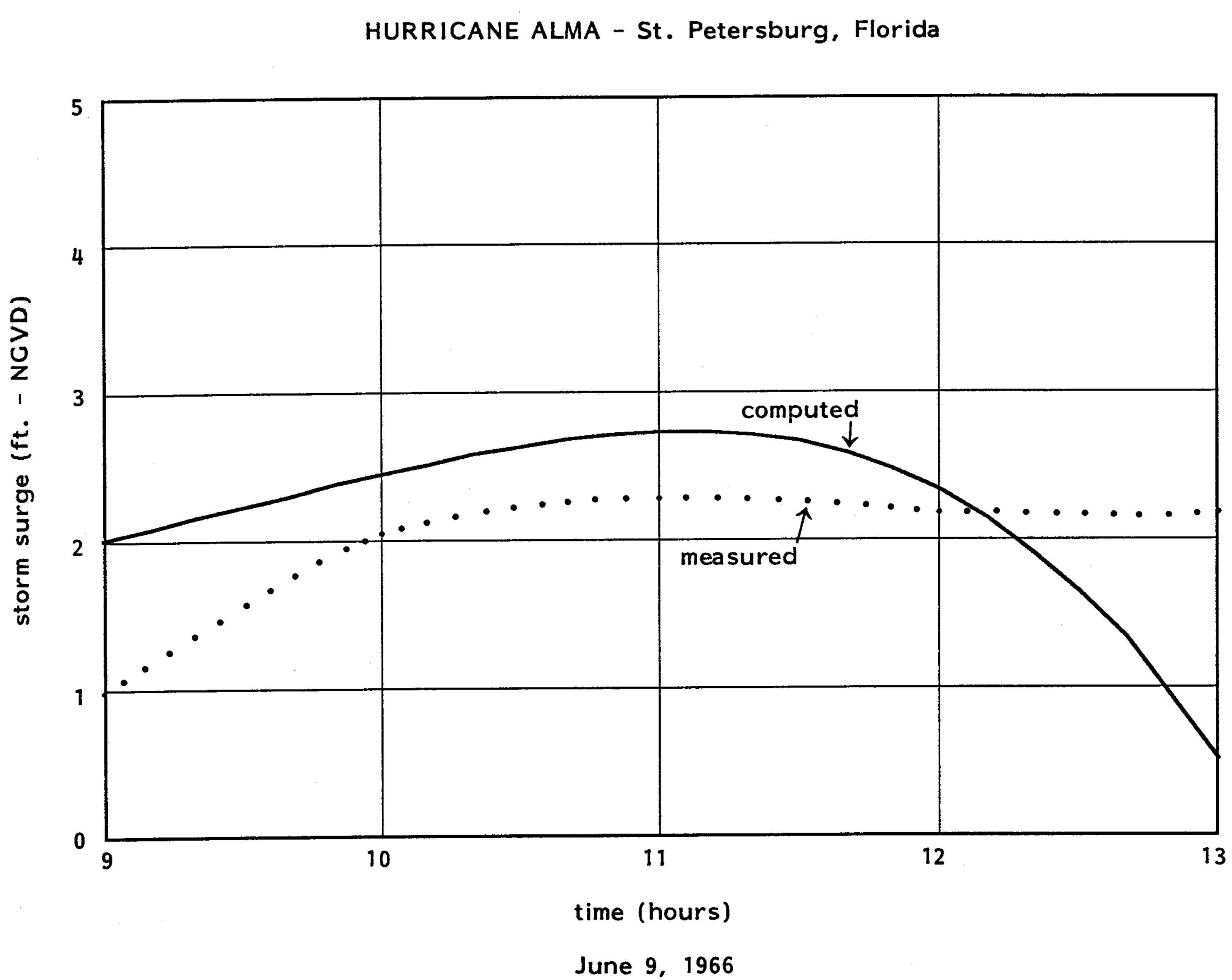

Figure 24 Comparison between Measured and Computed Storm Tide at St. Petersburg, Florida for Hurricane Alma, June 1966

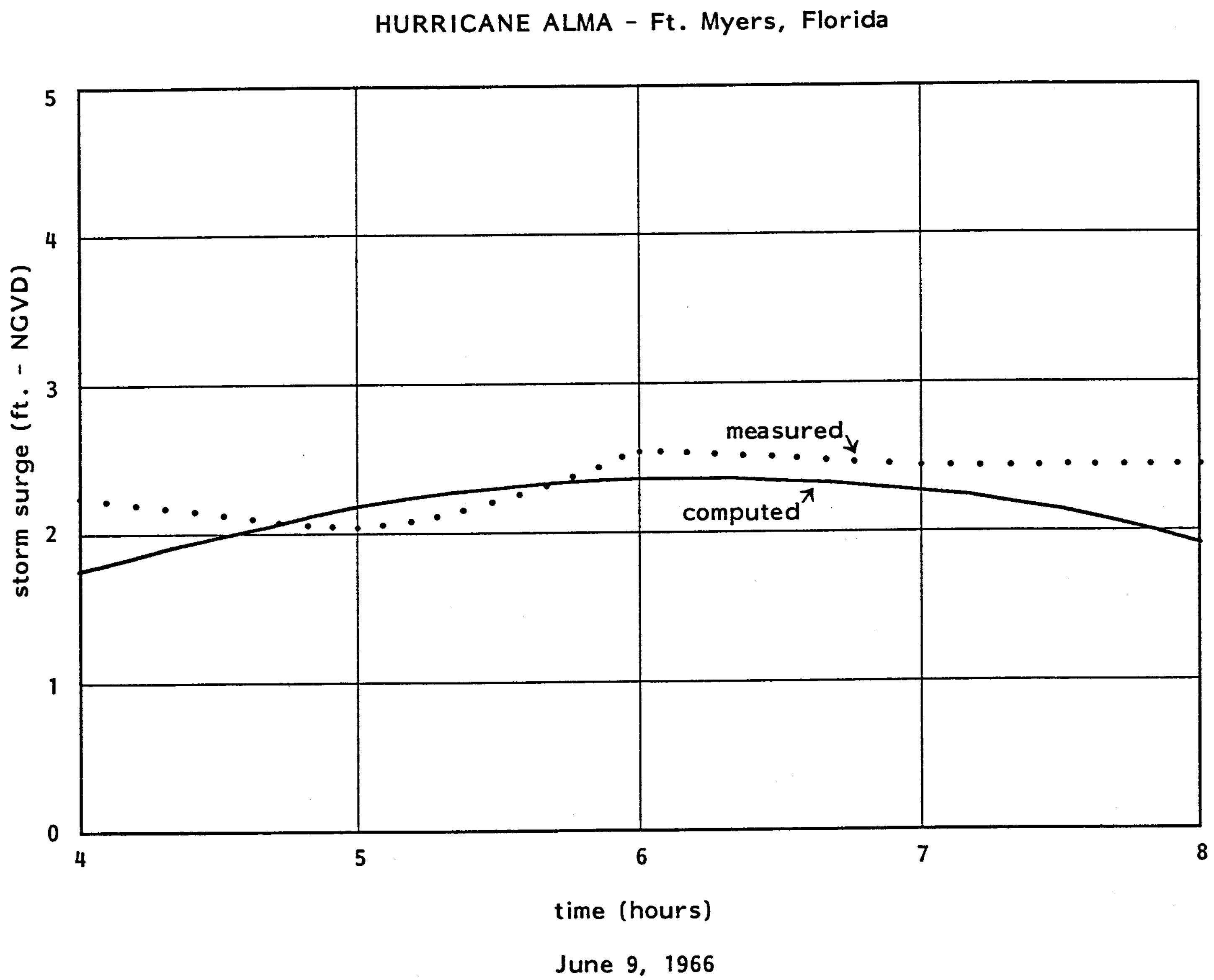

Figure 25 Comparison between Measured and Computed Storm Tide at Ft. Myers, Florida for Hurricane Alma, June 1966

TABLE IIa

Parameters Defining 11 Landfalling Model Hurricanes
Used In Calibrating The One-Dimensional Model
With The Two-Dimensional Model

MODEL STORM	Δp (in.Hg)	R (n. mi.)	V_F (knots)	θ_N (degrees)	Landfalling Coordinates (n. mi.)		Starting Coordinates (n. mi.)	
					X_F	Y_F	X_S	Y_S
1	-1.1	22	13	210	-20	+30	90.84	-37.93
2	-1.1	32	13	210	-20	+30	90.84	-37.93
3	-1.1	12	13	210	-20	+30	90.84	-37.93
4	-0.4	22	13	210	-20	+30	90.84	-37.93
5	-1.8	22	13	210	-20	+30	90.84	-37.93
6	-1.1	22	17	210	-20	+30	95.96	-41.06
7	-1.1	22	9	210	-20	+30	95.11	-40.54
8	-1.1	22	13	210	-20	+30	109.96	26.60
9	-1.1	22	13	210	-20	+30	42.03	-84.25
10	-1.1	22	13	210	-20	-10	90.84	-77.93
11	-1.1	22	13	210	-20	+70	90.84	2.07

TABLE IIb

Results of Calibration of Landfalling Model Hurricanes

Model Storm	η_{max} (ft. NGVD)					
	North Profile		Middle Profile		South Profile	
	1-D	2-D	1-D	2-D	1-D	2-D
1	6.94	7.76	9.12	10.04	8.43	9.37
2	7.35	8.39	9.60	10.87	10.02	11.19
3	6.73	7.17	7.51	8.19	5.74	6.39
4	4.46	4.71	6.36	6.67	5.67	5.99
5	9.53	10.84	12.21	13.65	11.46	12.86
6	7.08	7.50	9.63	10.28	8.99	9.60
7	6.77	7.21	8.59	9.41	7.87	8.88
8	9.54	11.04	8.90	10.68	7.30	8.94
9	5.76	6.54	7.04	7.86	8.11	8.13
10	1.48	1.60	2.35	3.00	4.27	5.21
11	7.40	8.61	5.96	7.33	4.96	6.15

TABLE IIIa

Parameters Defining 11 Alongshore Model Hurricanes
Used In Calibrating The One-Dimensional Model
With The Two-Dimensional Model

MODEL STORM	Δp (in.Hg)	R (n. mi.)	V_F (knots)	θ_N (degrees)	Landfalling Coordinates (n. mi.)		Starting Coordinates (n. mi.)	
					X_L	Y_L	X_S	Y_S
1	-0.9	22	11	150	+40	-12	37.12	-97.96
2	-0.9	32	11	150	+40	-12	37.12	-97.96
3	-0.9	12	11	150	+40	-12	37.12	-97.96
4	-0.5	22	11	150	+40	-12	37.12	-97.96
5	-1.3	22	11	150	+40	-12	37.12	-97.96
6	-0.9	22	15	150	+40	-12	36.86	-107.96
7	-0.9	22	7	150	+40	-12	37.25	-92.96
8	-0.9	22	11	160	+40	-12	56.26	-96.79
9	-0.9	22	11	140	+40	-12	18.07	-95.79
10	-0.9	22	11	150	+18	-12	15.12	-97.96
11	-0.9	22	11	150	+62	-12	59.12	-97.96

TABLE IIIb

Results of Calibration of Alongshore Model Hurricanes

Model Storm	η_{max} (ft. NGVD)					
	North Profile		Middle Profile		South Profile	
	1-D	2-D	1-D	2-D	1-D	2-D
1	2.94	3.34	2.90	3.40	3.05	3.56
2	3.98	4.45	3.93	4.50	4.10	4.69
3	1.72	1.94	1.69	2.02	1.80	2.11
4	2.02	2.16	1.99	2.19	2.08	2.33
5	3.91	4.54	3.85	4.64	4.06	4.80
6	3.11	3.79	3.06	3.76	3.21	3.66
7	2.77	3.07	2.73	3.00	2.88	2.89
8	3.65	4.11	3.38	4.00	3.33	3.96
9	2.32	2.58	2.47	2.81	2.81	3.19
10	5.22	5.32	5.09	5.47	5.29	5.67
11	1.69	2.32	1.69	2.37	1.78	2.44

TABLE IVa

Parameters Defining 11 Exiting Model Hurricanes
Used In Calibrating The One-Dimensional Model
With The Two-Dimensional Model

MODEL STORM	Δp (in.Hg)	R (n. mi.)	V_F (knots)	θ_N (degrees)	Landfalling Coordinates (n. mi.) X_E	Y_E	Starting Coordinates (n. mi.) X_S	Y_S
1	-1.1	22	11	100	+5	+15	-81.09	-53.48
2	-1.1	32	11	100	+5	+15	-81.09	-53.48
3	-1.1	12	11	100	+5	+15	-81.09	-53.48
4	-0.4	22	11	100	+5	+15	-81.09	-53.48
5	-1.8	22	11	100	+5	+15	-81.09	-53.48
6	-1.1	22	15	100	+5	+15	-88.91	-59.70
7	-1.1	22	7	100	+5	+15	-77.17	-50.36
8	-1.1	22	11	80	+5	+15	-99.32	-19.90
9	-1.1	22	11	120	+5	+15	-52.47	-78.79
10	-1.1	22	11	100	+5	-10	-81.09	-78.48
11	-1.1	22	11	100	+5	+40	-81.09	-28.48

TABLE IVb

Results of Calibration of Exiting Model Hurricanes

Model Storm	η_{max} (ft. NGVD)					
	North Profile		Middle Profile		South Profile	
	1-D	2-D	1-D	2-D	1-D	2-D
1	3.80	3.46	6.31	5.89	6.83	6.52
2	4.01	3.79	6.25	5.90	7.59	7.18
3	3.31	2.91	6.15	5.76	4.85	4.67
4	1.85	1.73	3.56	3.45	3.86	3.79
5	5.87	5.40	9.15	8.43	9.81	9.25
6	3.77	3.74	6.17	5.85	6.59	6.42
7	3.81	3.49	6.42	6.02	7.03	6.59
8	1.89	1.63	6.28	5.70	6.49	6.12
9	5.65	5.29	6.67	6.52	7.18	7.00
10	0.95	1.08	2.01	1.96	4.60	4.18
11	7.02	6.55	6.14	5.95	5.03	4.95

dimensional numerical model and those from the two-dimensional model is determined as follows. The peak surges computed from these two models are plotted as shown in Figures 26a, 26b, 27a, 27b, 28a and 28b. Figures 26a and 26b are for landfalling hurricanes at the north, middle and south transect line, respectively. Correspondingly, Figures 27a and 27b are for alongshore hurricanes and Figures 28a and 28b are for exiting hurricanes. The relationship between the two computed values are represented by the straight lines in the plots.

In summary, the overall calibration procedure for the simulation is that presented in Figure 14. Eleven cases each for the landfalling, alongshore and exiting hurricanes with parameters encompassing representative ranges of their cumulative probability distributions are chosen. Peak storm surges corresponding to three locations along the Sarasota County shoreline (Figure 15) are calculated for the same 33 hurricanes by both one-dimensional and two-dimensional numerical models. Then, for each of the three transect lines, the calculated peak surges are correlated to establish the relationship between the one-dimensional and two-dimensional results. This "calibrated" storm surge relationship for each of the three transect lines is then utilized in the simulation as described previously to establish a combined total storm tide. The peak of the combined total storm tide is the value at the site which is later ranked with 632 other similarly-determined peaks to establish the combined total storm tides associated with various return periods of interest.

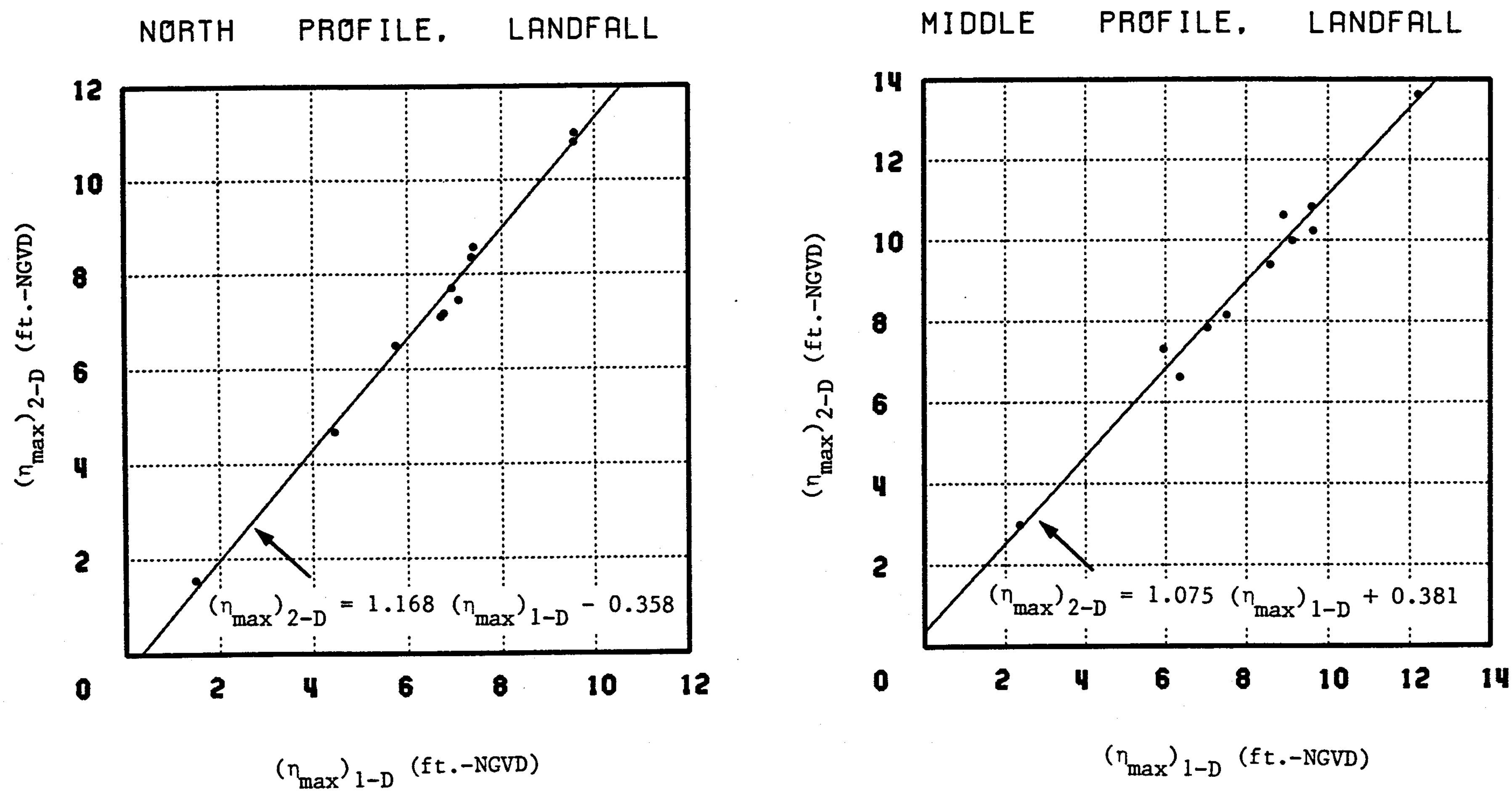

Figure 26a Calibration Relationship between the One-Dimensional and the Two-Dimensional Calculations of Peak Surges at the North and Middle Transect Lines of Sarasota County for Landfalling Hurricanes

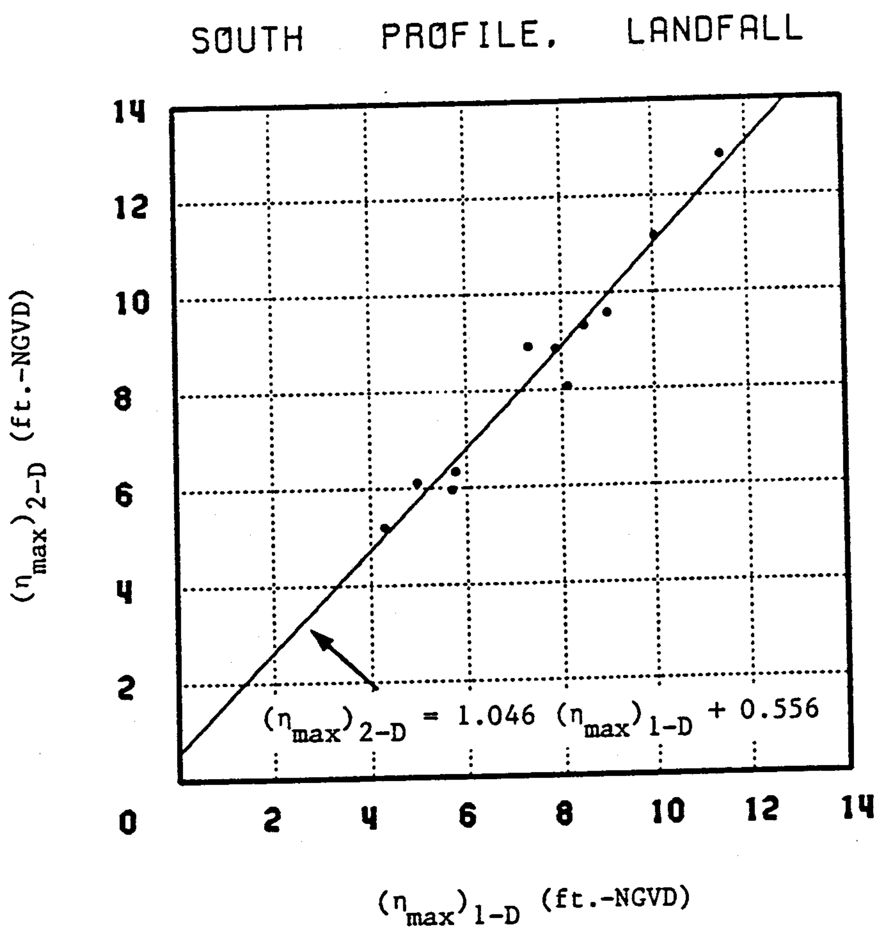

Figure 26b Calibration Relationship between the One-Dimensional and the Two-Dimensional Calculations of Peak Surges at the South Transect Line of Sarasota County for Landfalling Hurricanes

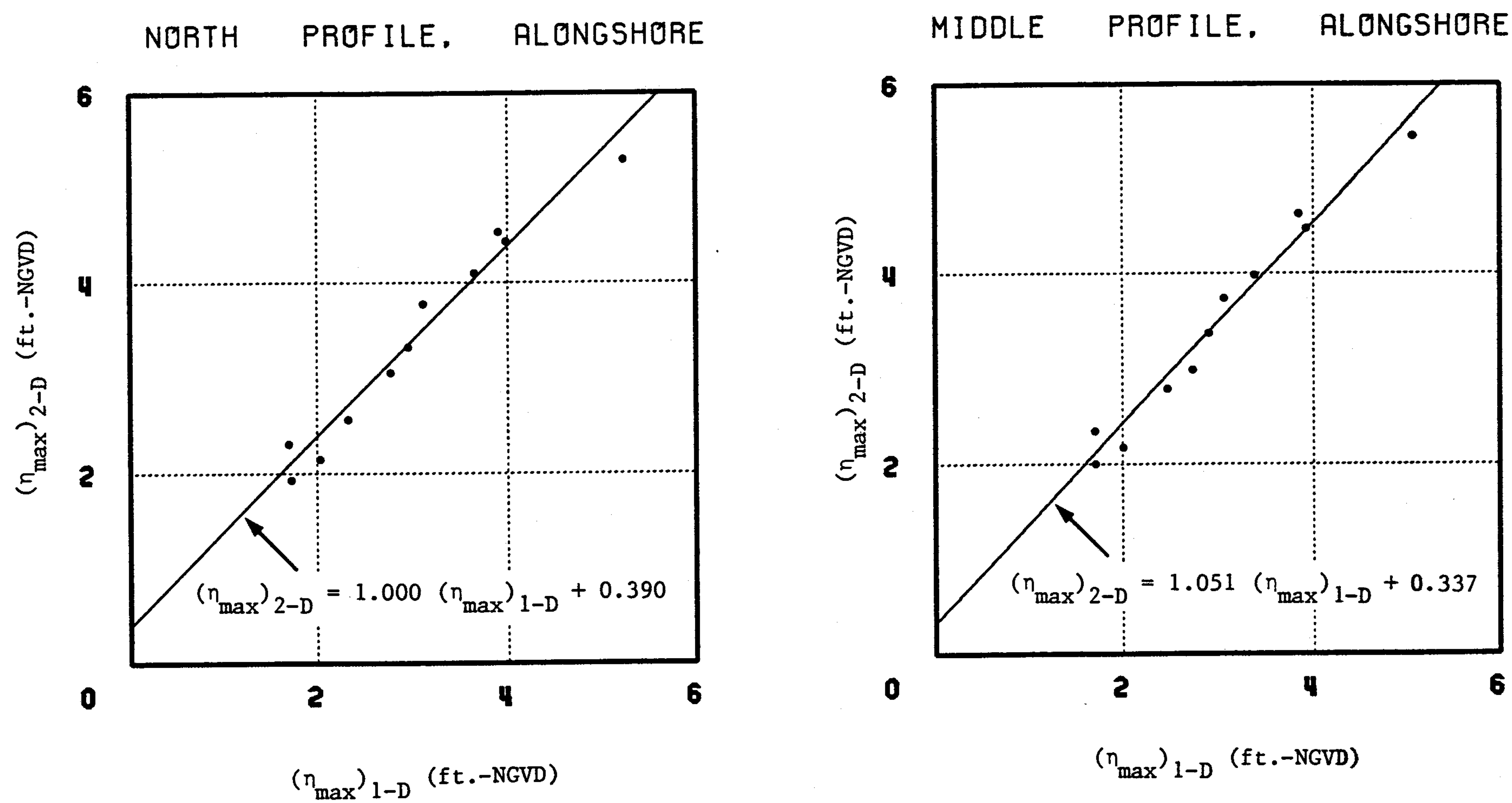

Figure 27a Calibration Relationship between the One-Dimensional and the Two-Dimensional Calculations of Peak Surges at the North and Middle Transect Lines of Sarasota County for Alongshore Hurricanes

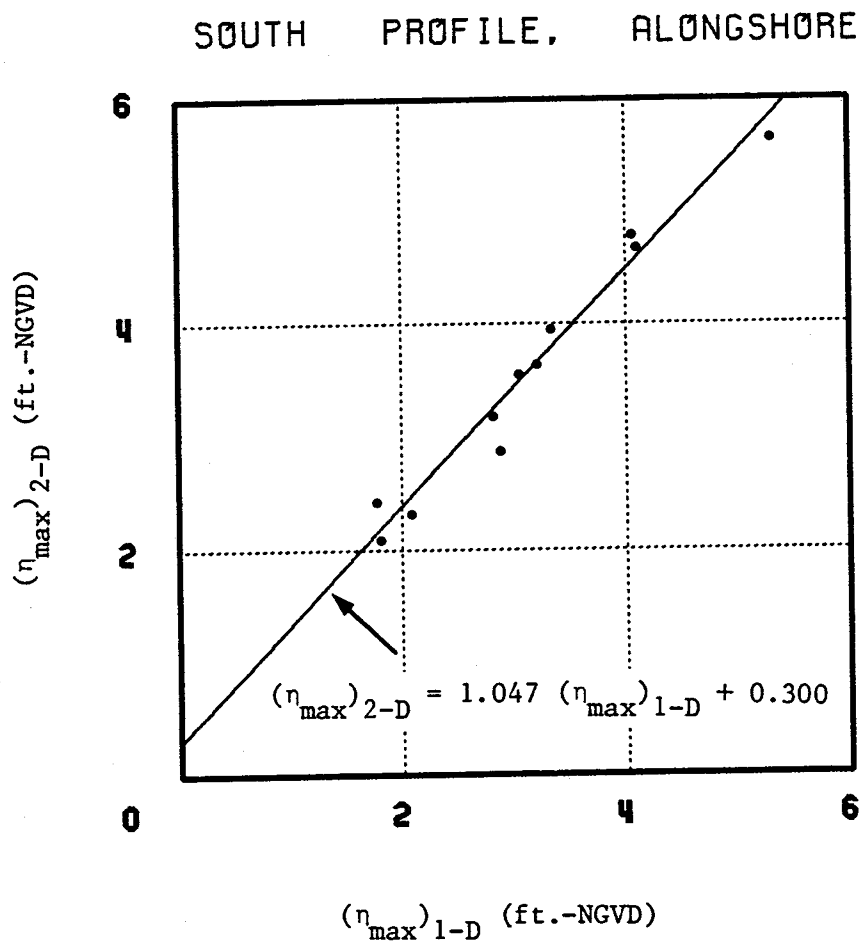

Figure 27b Calibration Relationship between the One-Dimensional and the Two-Dimensional Calculations of Peak Surges at the South Transect Line of Sarasota County for Alongshore Hurricanes

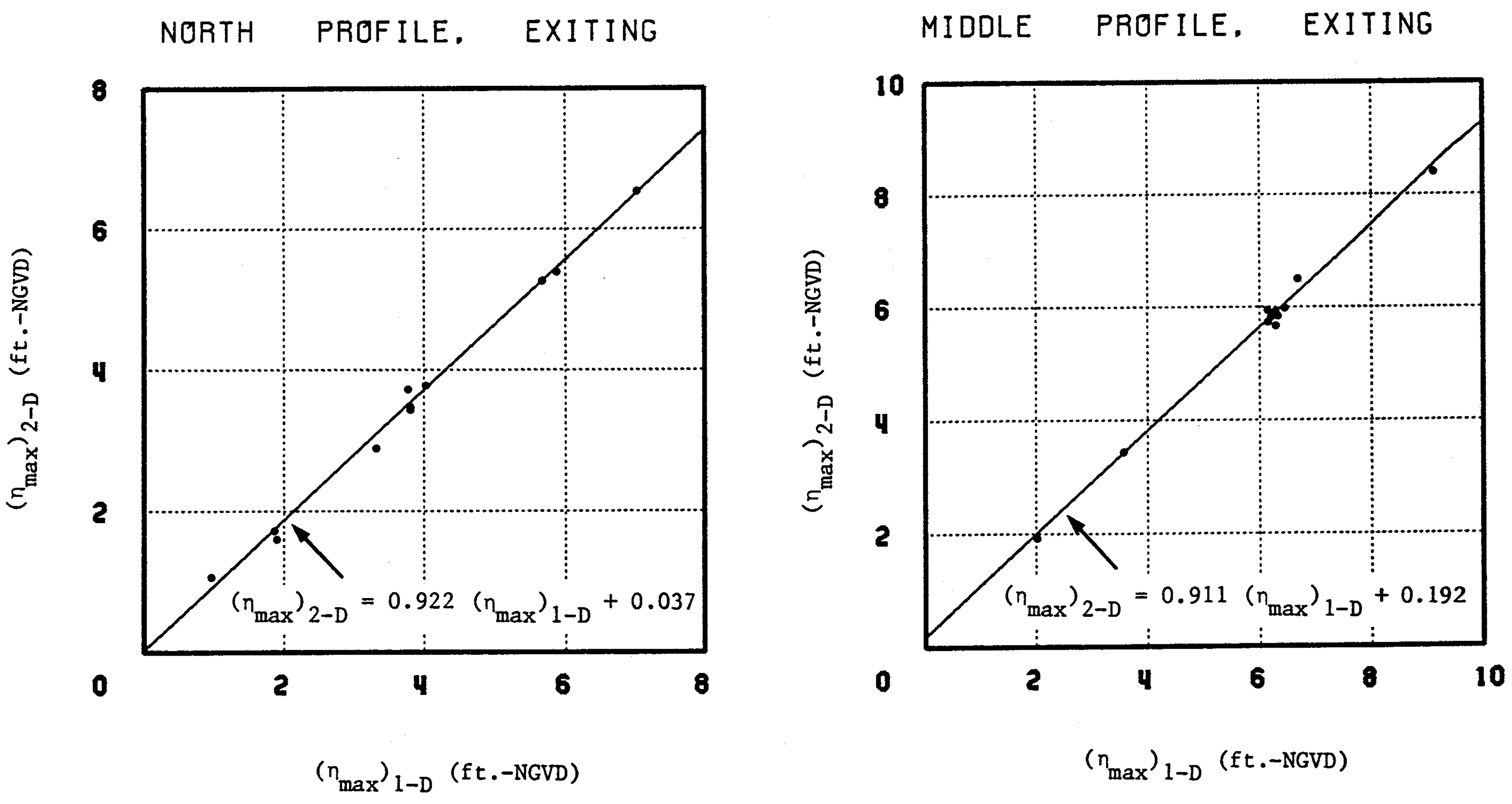

Figure 28a Calibration Relationship between the One-Dimensional and the Two-Dimensional Calculations of Peak Surges at the North and Middle Transect Lines of Sarasota County for Exiting Hurricanes

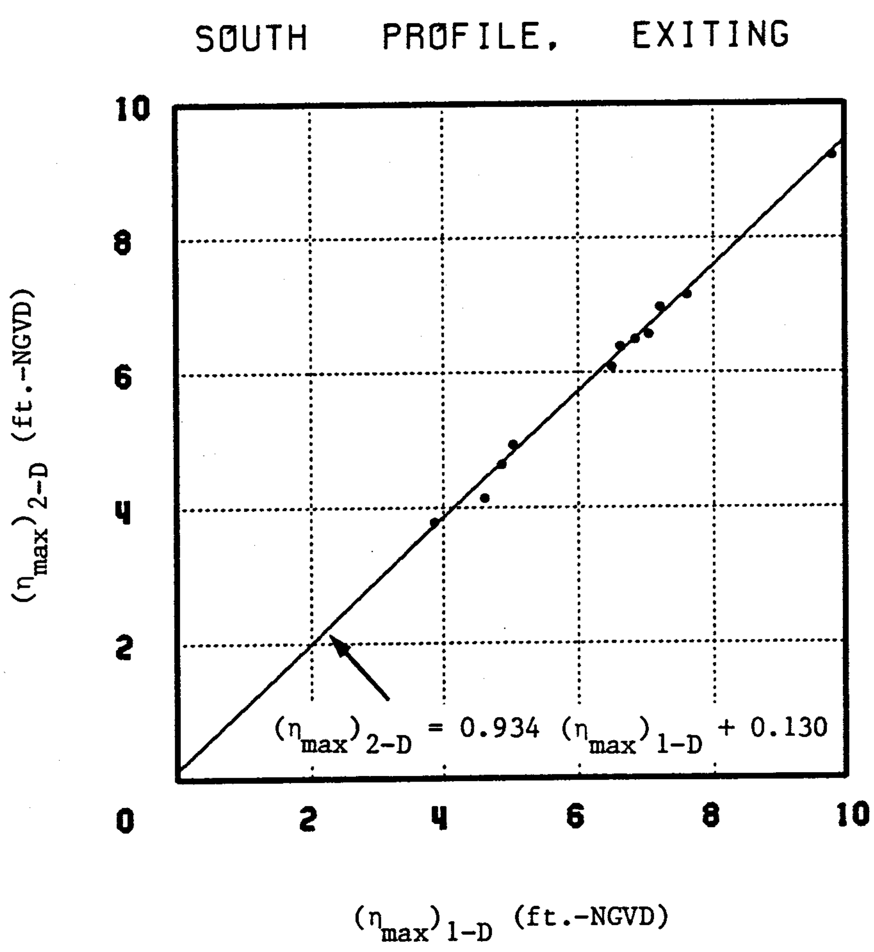

Figure 28b Calibration Relationship between the One-Dimensional and the Two-Dimensional Calculations of Peak Surges at the South Transect Line of Sarasota County for Exiting Hurricanes

VI. RESULTS OF LONG-TERM SIMULATIONS

Five 2,000-year simulations for each of the three transect lines are carried out employing the computer methods and hurricane statistics presented in the preceding sections. The combined total storm tides above NGVD and the associated return periods computed from Equation 27 are plotted on semi-log paper in Figures 29a, 29b and 29c, respectively for the three transect line locations along the Sarasota County shoreline. Each data point on these three figures represents the average value of five simulations and a curve drawn through the data points is adopted to represent the tide-frequency relationship for each of the three transect lines. Figure 30 presents all three combined total storm tide frequency curves depicted in Figures 29a, 29b and 29c.

Table V below gives the combined total storm tide values and corresponding return periods for the three transect lines.

Table V

Combined Total Storm Tide Values for Various Return Periods

Return Period, TR (years)	Combined Total Storm Tide Level* above NGVD (ft)		
	North Profile	Middle Profile	South Profile
500	16.0	15.6	15.5
200	14.4	14.0	14.2
100	12.9	12.6	12.8
50	11.4	11.3	11.4
20	8.7	8.8	8.9
10	5.7	6.0	6.2

*Includes contributions of: wind stress, barometric pressure, dynamic wave setup and astronomical tide.

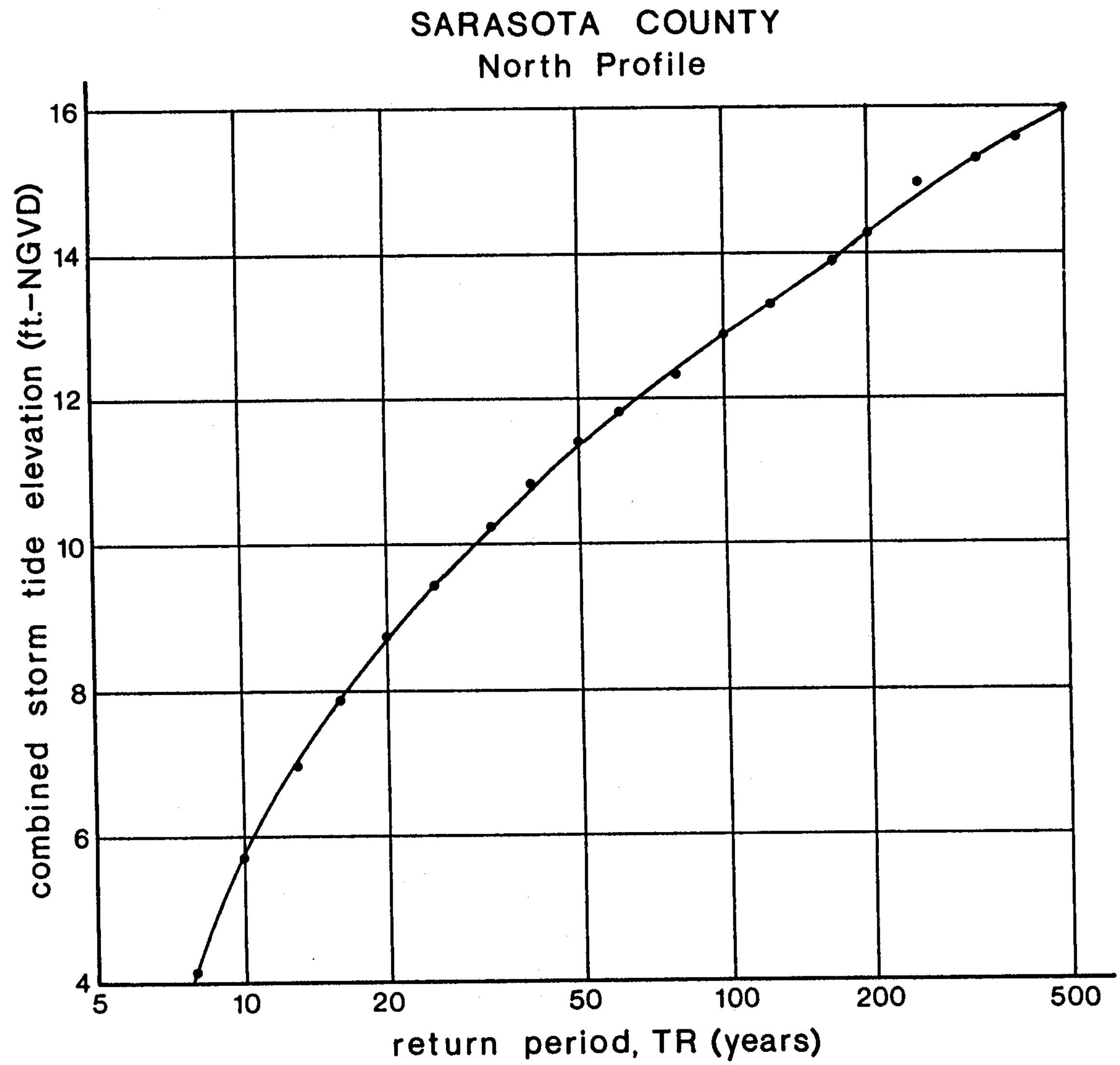

Figure 29a Results of Five 2,000-Year Simulations for North Transect Line in Sarasota County

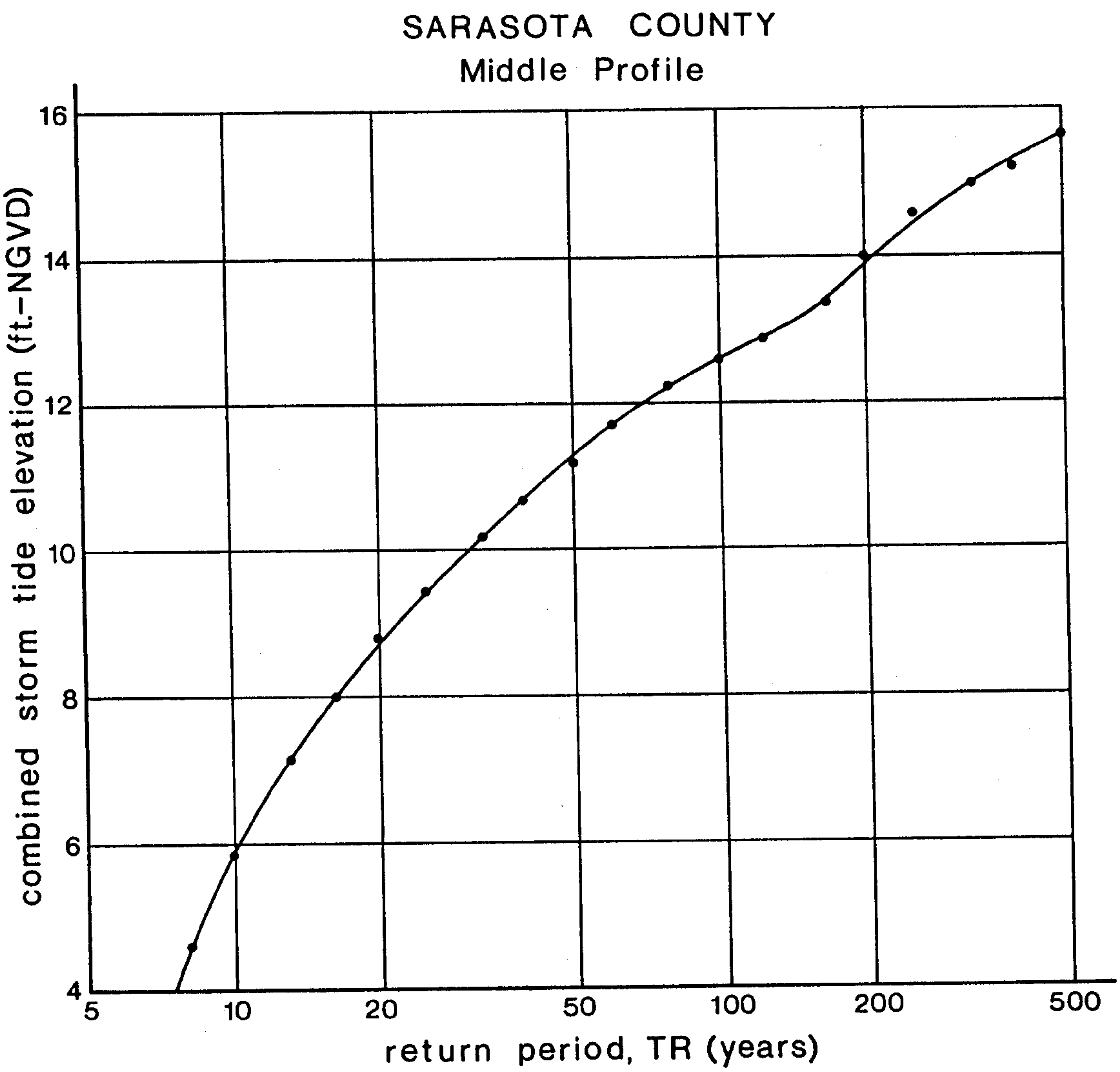

Figure 29b Results of Five 2,000-Year Simulations for Middle Transect Line in Sarasota County

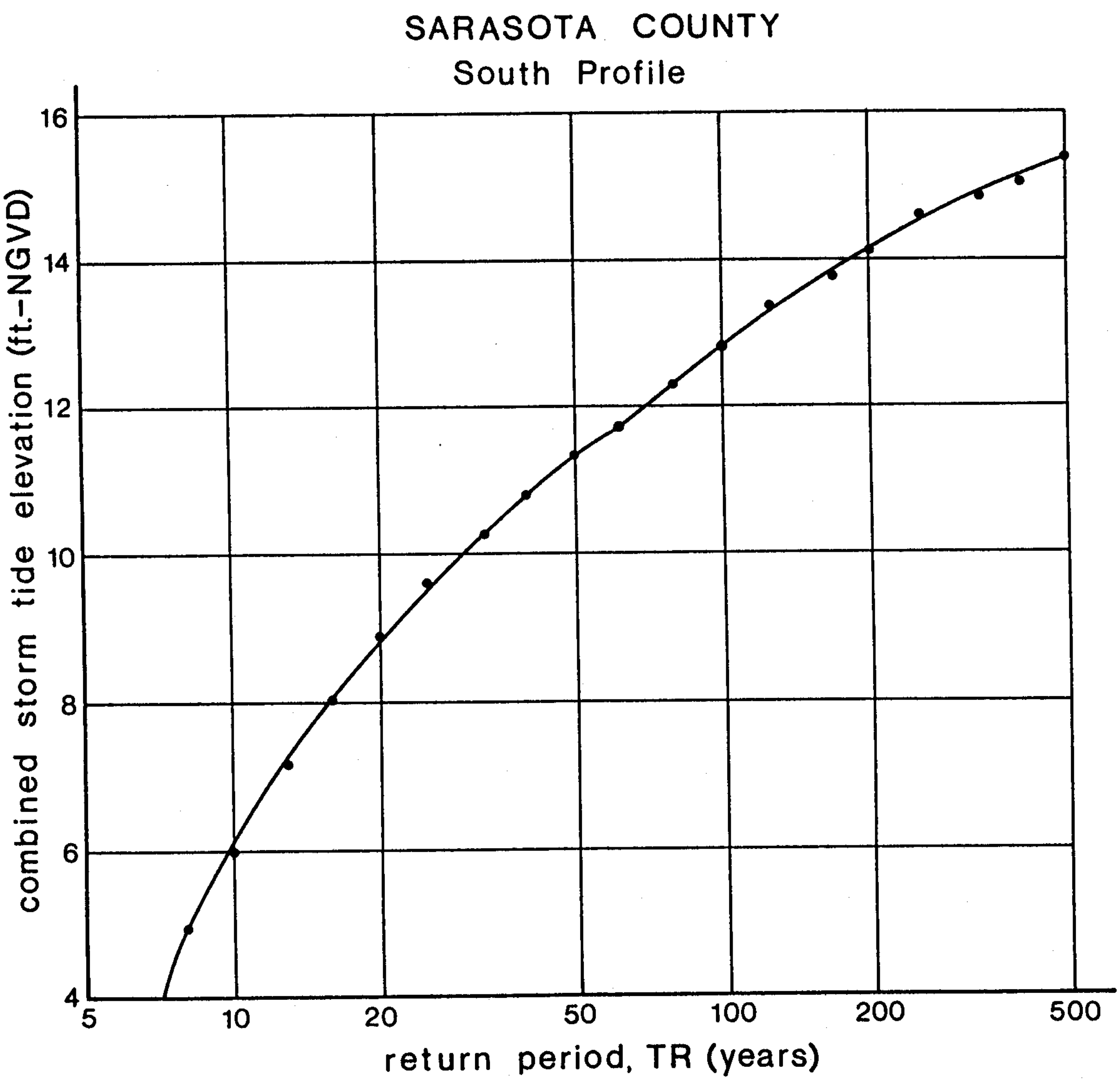

Figure 29c Results of Five 2,000-Year Simulations for South Transect Line in Sarasota County

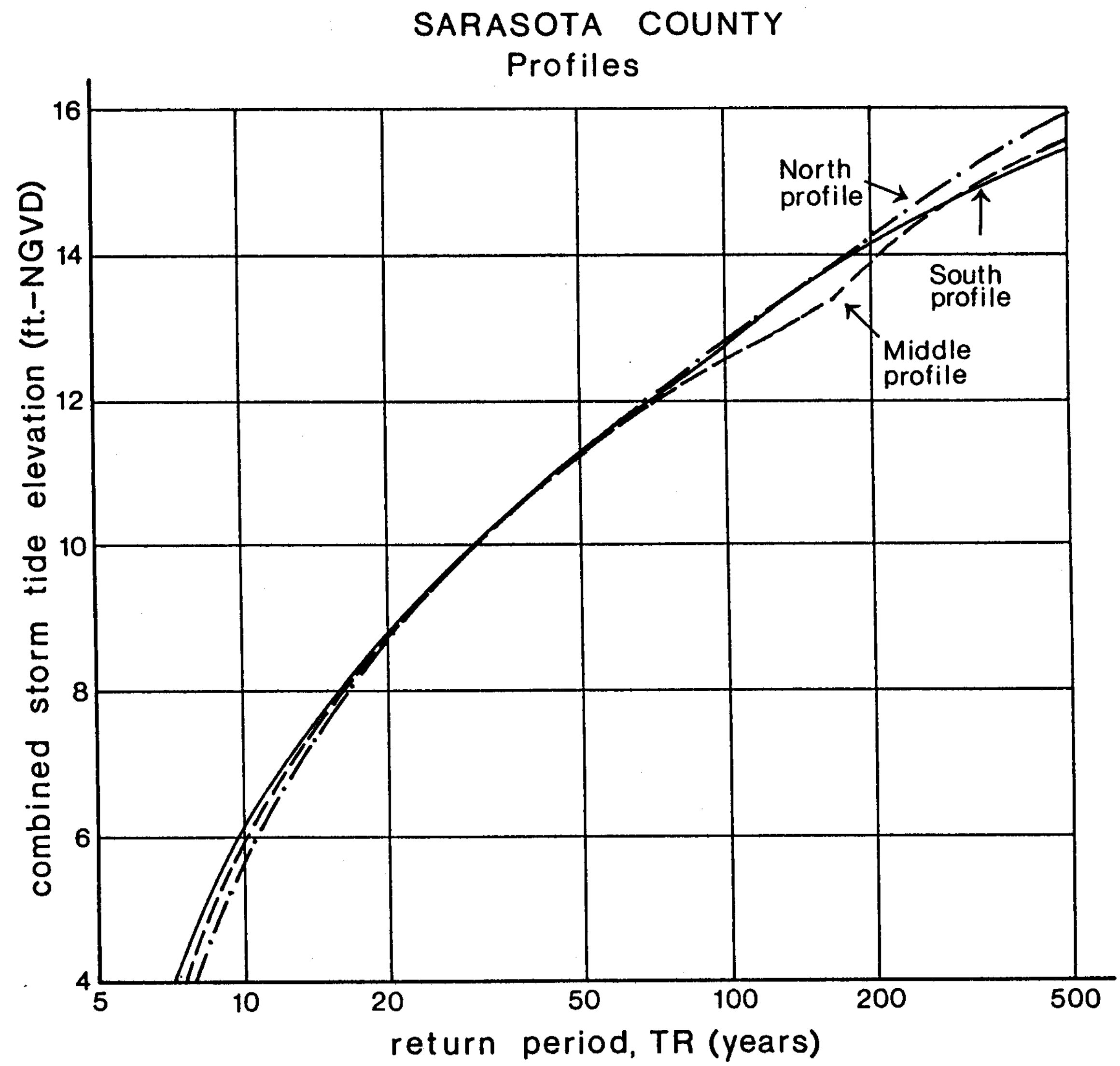

Figure 30 Combined Total Storm Tide Elevation Versus Return Period for Three Transect LInes in Sarasota County

For the purpose of other applications, the selected 100 year frequency storm hydrographs are provided in Appendix C. Table CI and Figure CI is for transect line 1 (north profile), Table CII and Figure CII for transect line 2 (middle profile) and Table CIII and Figure CIII for transect line 3 (south profile) in Sarasota County.

REFERENCES

1. U. S. Army Corps of Engineers, "National Shoreline Study - Regional Inventory Report," South Atlantic Division, Atlanta, Georgia, August 1971.

2. U. S. Army Corps of Engineers, "Beach Erosion Control Study for Sarasota County, Florida with Environmental Impact Statement," Jacksonville District, Jacksonville, Florida, 1984.

3. U. S. Department of Commerce, National Oceanic and Atmospheric Administration, "Meteorological Criteria for Standard Project Hurricane and Probable Maximum Hurricane Windfields, Gulf and East Coasts of the United States," NOAA Technical Report NWS 23, September 1979.

4. U. S. Department of Commerce, National Oceanic and Atmospheric Administration, National Weather Service, "Hurricanes Affecting Manatee, Sarasota, and Charlotte Counties, Florida," 1973.

5. Wilson, B. L., "Hurricane Wave Statistics for the Gulf of Mexico," U. S. Army Corps of Engineers, Beach Erosion Board, Technical Memorandum 98, 1956.

6. Van Dorn, W., "Wind Stress on an Artificial Pond," Journal of Marine Research, Volume 12, No. 3, 1953.

7. Christensen, B. A. and Walton, R., "Friction Factors in Flooding Due to Hurricanes," Proceedings, National Symposium on Urban Stormwater Management in Coastal Area, Blacksburg, Virginia, June 19-20, 1980.

8. Saville, T., "Experimental Determination of Wave Set-Up," Proceedings, Second Technical Conference on Hurricanes, pp. 242-252, 1961.

9. Bowen, A. J., Inman, D. L. and Simmons, V. P., "Wave 'Set-Down and Set-Up'," Journal of Geophysical Research, Volume 73, No. 8, pp. 2569-2577, 1968.

10. Lo, J. M., "Dynamic Wave Setup," Paper No. 111, 21st International Conference on Coastal Engineering, Malaga, Spain, June 1988.

11. U. S. Army Corps of Engineers, "Shore Protection Manual, Volumes I, II and III," U. S. Government Printing Office, 1984.

APPENDIX A

SARASOTA COUNTY

#	Date	θ_N (degrees)	Y_F (n.mi.)	V_F (knots)	Δp (in Hg)	R (n.mi.)	Remarks
1	06/17/1906	185.0	-141.0	10.0	-1.00	26.0	
2	10/18/1906	230.0	-141.0	6.0	-0.99	35.0	
3	10/11/1909	235.0	-146.0	10.0	-1.54	22.0	
4	10/18/1910	200.0	-76.0	11.0	-1.97	16.0	
5	09/10/1919	110.0	-96.0	8.0	-2.44	15.0	
6	10/25/1921	235.0	54.0	10.0	-1.71	18.0	
7	10/21/1924	250.0	-96.0	8.0	-1.18	19.0	
8	09/11/1926	119.0	-46.0	12.0	-1.86	17.0	
9	09/17/1928	120.0	34.0	12.0	-1.58	MSG	
10	09/21/1929	138.0		8.0	-1.11	MSG	
11	09/04/1933	120.0	39.0	11.0	-1.40	29.0	
12	11/05/1935	65.0	-141.0	15.0	-1.27	10.0	
13	10/03/1941	128.0	-47.0	18.0	-1.02	18.0	
14	10/19/1944	195.0	-6.0	13.0	-1.86	27.0	
15	09/18/1947	85.0	-91.0	7.0	-1.97	34.0	
16	09/21/1948	210.0	-126.0	8.0	-2.21	7.0	
17	10/05/1948	230.0	-131.0	13.0	-0.98	31.0	
18	08/27/1949	130.0	4.0	14.0	-1.60	23.0	
19	09/05/1950 (Easy)	230.0	104.0	3.0	-1.50	15.0	
20	10/18/1950 (King)	150.0		17.0	-1.06	MSG	
21	09/10/1960 (Donna)	171.0		9.0	-2.43	20.0	
22	10/14/1964 (Isbell)	220.0	-96.0	15.0	-1.44	10.0	
23	09/08/1965 (Betsy)	90.0	-121.0	15.0	-1.92	19.0	
24	06/04/1966 (Alma)	159.0		17.0	-1.15	23.0	
25	10/19/1968 (Gladys)	235.0	114.0	10.0	-1.01	21.0	

APPENDIX B

HURRICANE MODEL

The idealized hurricane model moving at a constant speed V_F at an angle, θ', with respect to the x-axis of the grid system is shown below. The gradient

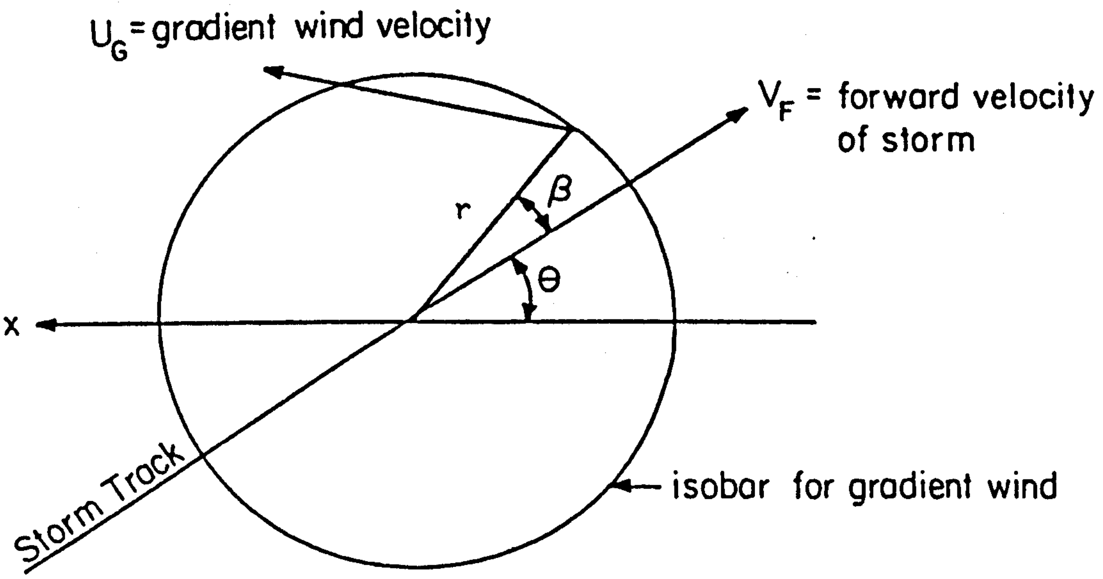

wind speed, U_G (wind speed at 30 ft. above water surface), is calculated by

$$U_G = U_c\left(\sqrt{\gamma^2 + 1} - \gamma\right) \cdot (0.83)$$

where

$$\gamma = \frac{1}{2}\left(\frac{V'}{U_c} + \frac{U_c}{U_g}\right)$$

and

$$U_c = \sqrt{\frac{\Delta p}{\rho_a}\frac{R}{r} e^{-R/r}}$$

$$U_g = \frac{\frac{\Delta p}{\rho_a}\frac{R}{r^2} e^{-R/r}}{2\omega(\sin\phi)}$$

$2\omega(\sin\phi)$ = coriolis effect

ω = earth rotation

ϕ = latitude

R = radius to maximum winds

$V' = V_F \sin\beta$

β = angle between observer and hurricane direction

V_F = constant translational speed of hurricane

ρ_a = mass density of air

r = distance from hurricane center to observer

U_g = geostrophic velocity component

U_c = cyclostrophic velocity component.

The factor of 0.83 was applied to the calculation of U_G to take into account friction effects at 30 feet above the water surface.

APPENDIX C

TABLE CI

100 Year Frequency Combined Total Storm Tide Hydrograph
for North Profile (Range 1 - Range 60)

TIME (hr.)	TIDE ELEVATION (ft.)
0.00	1.25
0.50	0.96
1.00	0.69
1.50	0.45
2.00	0.24
2.50	0.07
3.00	-0.04
3.50	-0.09
4.00	-0.07
4.50	0.00
5.00	0.10
5.50	0.22
6.00	0.37
6.50	0.54
7.00	0.73
7.50	0.73
8.00	1.05
8.50	1.40
9.00	1.80
9.50	2.23
10.00	2.70
10.50	3.22
11.00	3.78
11.50	4.40
12.00	5.06
12.50	5.76
13.00	6.52
13.50	7.32
14.00	8.15
14.50	8.99
15.00	9.83
15.50	10.62
16.00	11.34
16.50	11.94
17.00	12.39
17.50	12.67
18.00	12.77
18.50	12.71
19.00	12.50
19.50	12.17
20.00	11.76
20.50	11.29
21.00	10.77
21.50	10.19
22.00	9.55

TIME (hr.)	TIDE ELEVATION (ft.)
22.50	8.87
23.00	8.16
23.50	7.44
24.00	6.71
24.50	5.98
25.00	5.27
25.50	4.59
26.00	3.95
26.50	3.36
27.00	2.84
27.50	2.38
28.00	2.00
28.50	1.70
29.00	1.49
29.50	1.32
30.00	1.19
30.50	1.09
31.00	1.01
31.50	0.96
32.00	0.93
32.50	0.93
33.00	0.95
33.50	0.99
34.00	1.04
34.50	1.12
35.00	1.20
35.50	1.30
36.00	1.41

TABLE CII

100 Year Frequency Combined Total Storm Tide Hydrograph for Middle Profile (Range 61 - Range 120)

TIME (hr.)	TIDE ELEVATION (ft.)
0.00	2.93
0.50	2.99
1.00	3.01
1.50	2.99
2.00	2.92
2.50	2.81
3.00	2.66
3.50	2.47
4.00	2.27
4.50	2.06
5.00	1.85
5.50	1.65
6.00	1.46
6.50	1.31
7.00	1.19
7.50	1.13
8.00	1.12
8.50	1.18
9.00	1.29
9.50	1.44
10.00	1.42
10.50	1.69
11.00	2.00
11.50	2.36
12.00	2.78
12.50	3.26
13.00	3.82
13.50	4.46
14.00	5.20
14.50	6.06
15.00	7.05
15.50	8.17
16.00	9.38
16.50	10.60
17.00	11.67
17.50	12.39
18.00	12.62
18.50	12.37
19.00	11.76
19.50	10.97
20.00	10.14
20.50	9.34
21.00	8.63
21.50	8.01
22.00	7.47
22.50	7.01
23.00	6.61
23.50	6.26
24.00	5.95
24.50	5.67
25.00	5.42
25.50	5.19
26.00	4.96
26.50	4.68
27.00	4.37
27.50	4.03
28.00	3.66
28.50	3.26
29.00	2.86
29.50	2.44
30.00	2.04
30.50	1.65
31.00	1.29
31.50	0.97
32.00	0.69
32.50	0.47
33.00	0.32
33.50	0.22
34.00	0.18
34.50	0.16
35.00	0.16
35.50	0.18
36.00	0.21

S

TABLE CIII

100 Year Frequency Combined Total Storm Tide Hydrograph
for South Profile (Range 121 - Range 183)

TIME (hr.)	TIDE ELEVATION (ft.)	TIME (hr.)	TIDE ELEVATION (ft.)
0.00	0.77	22.50	6.48
0.50	0.42	23.00	5.86
1.00	0.10	23.50	5.25
1.50	-0.20	24.00	4.67
2.00	-0.46	24.50	4.11
2.50	-0.67	25.00	3.59
3.00	-0.84	25.50	3.12
3.50	-0.94	26.00	2.69
4.00	-1.01	26.50	2.32
4.50	-1.07	27.00	2.01
5.00	-1.10	27.50	1.77
5.50	-1.13	28.00	1.60
6.00	-1.14	28.50	1.49
6.50	-1.14	29.00	1.40
7.00	-1.12	29.50	1.33
7.50	-1.08	30.00	1.28
8.00	-1.01	30.50	1.26
8.50	-0.91	31.00	1.25
9.00	-0.78	31.50	1.26
9.50	-0.59	32.00	1.29
10.00	-0.37	32.50	1.34
10.50	-0.08	33.00	1.40
11.00	0.24	33.50	1.47
11.50	0.63	34.00	1.56
12.00	1.04	34.50	1.65
12.50	1.49	35.00	1.76
13.00	1.99	35.50	1.87
13.50	2.54	36.00	1.98
14.00	3.15		
14.50	3.84		
15.00	4.63		
15.50	5.49		
16.00	7.06		
16.50	9.13		
17.00	10.85		
17.50	12.30		
18.00	12.80		
18.50	12.36		
19.00	11.56		
19.50	10.70		
20.00	9.90		
20.50	9.16		
21.00	8.45		
21.50	7.78		
22.00	7.12		

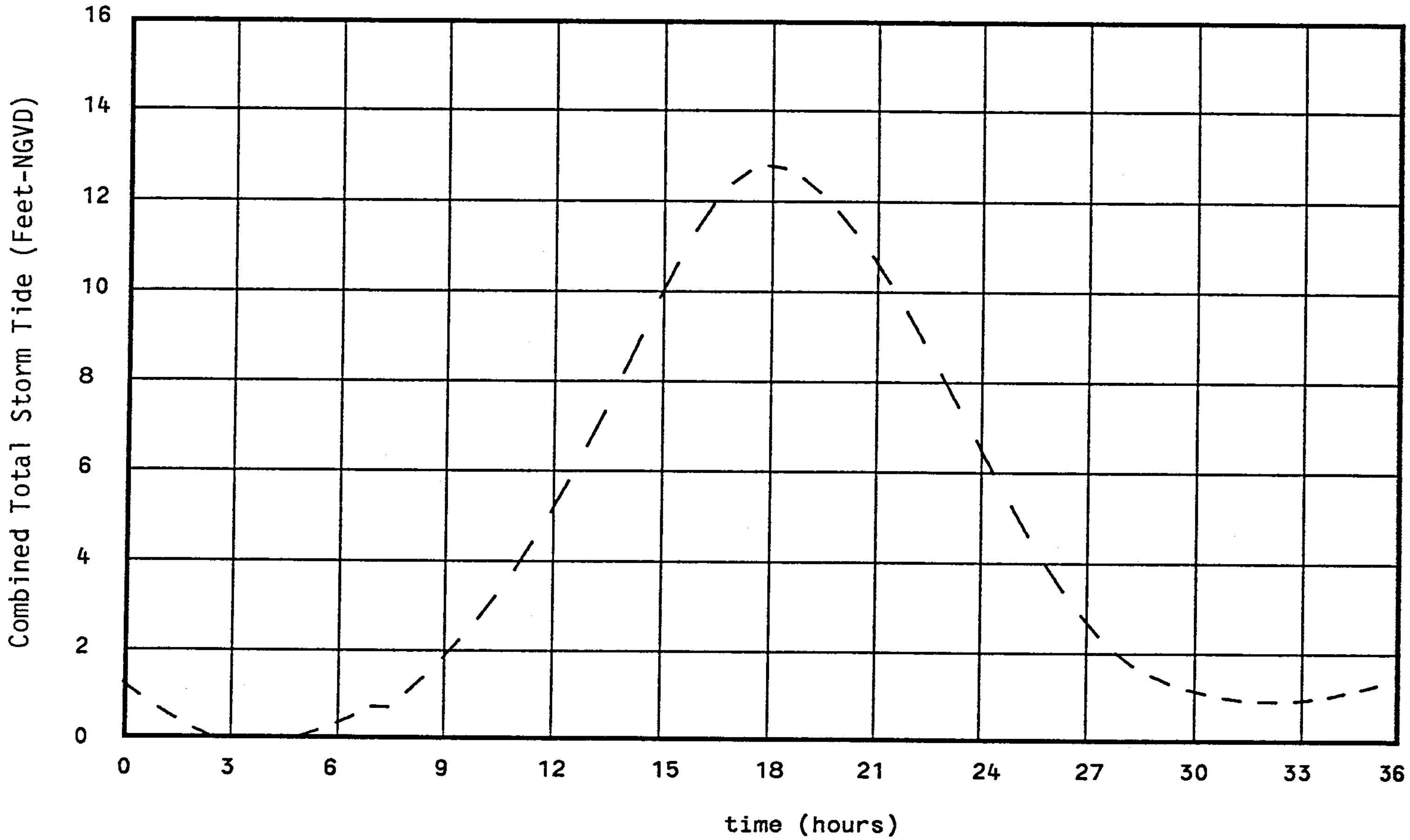

Figure CI 100 Year Frequency Combined Total Storm Tide Hydrograph for North Profile

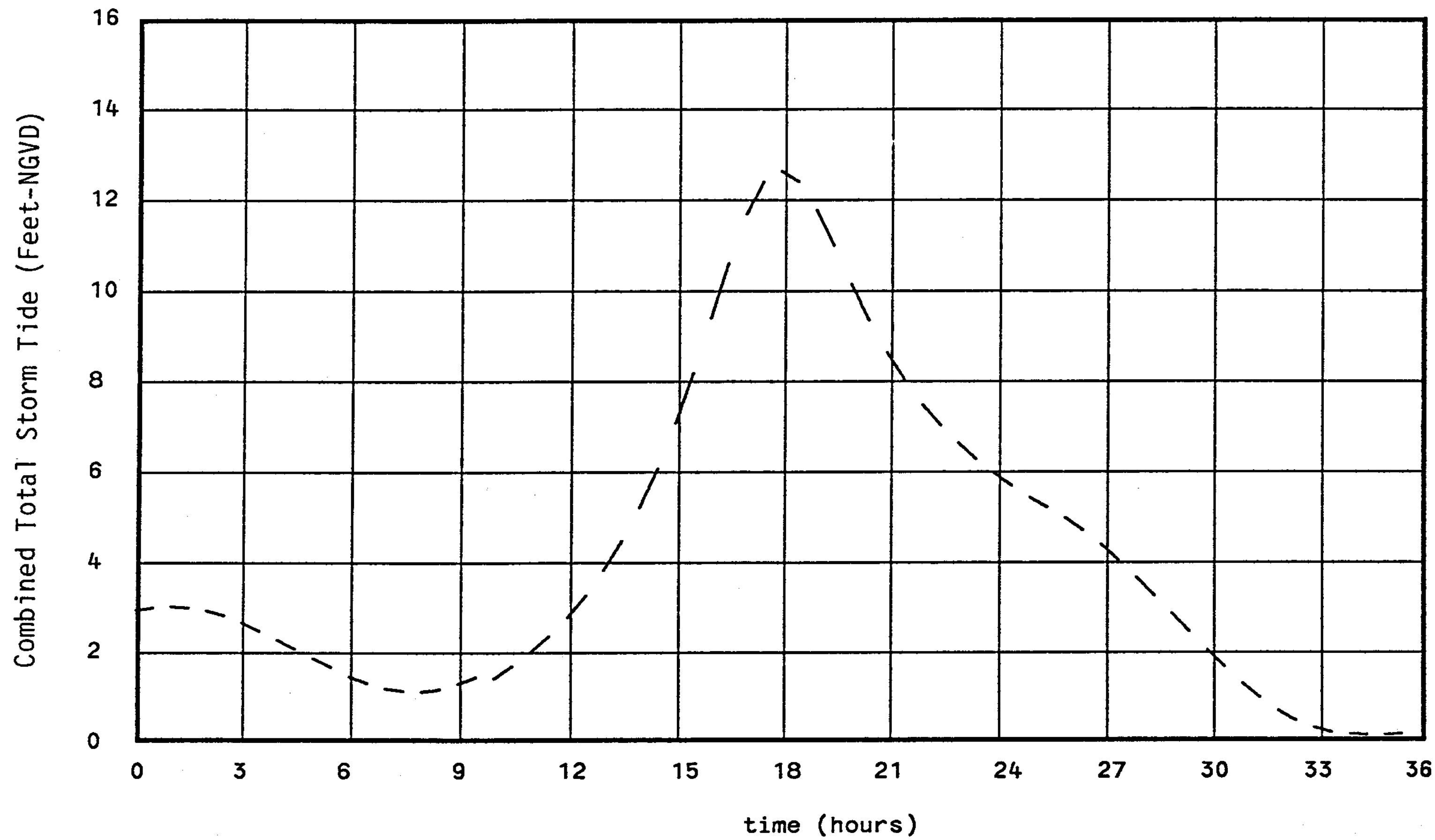

Figure CII 100 Year Frequency Combined Total Storm Tide Hydrograph for Middle Profile

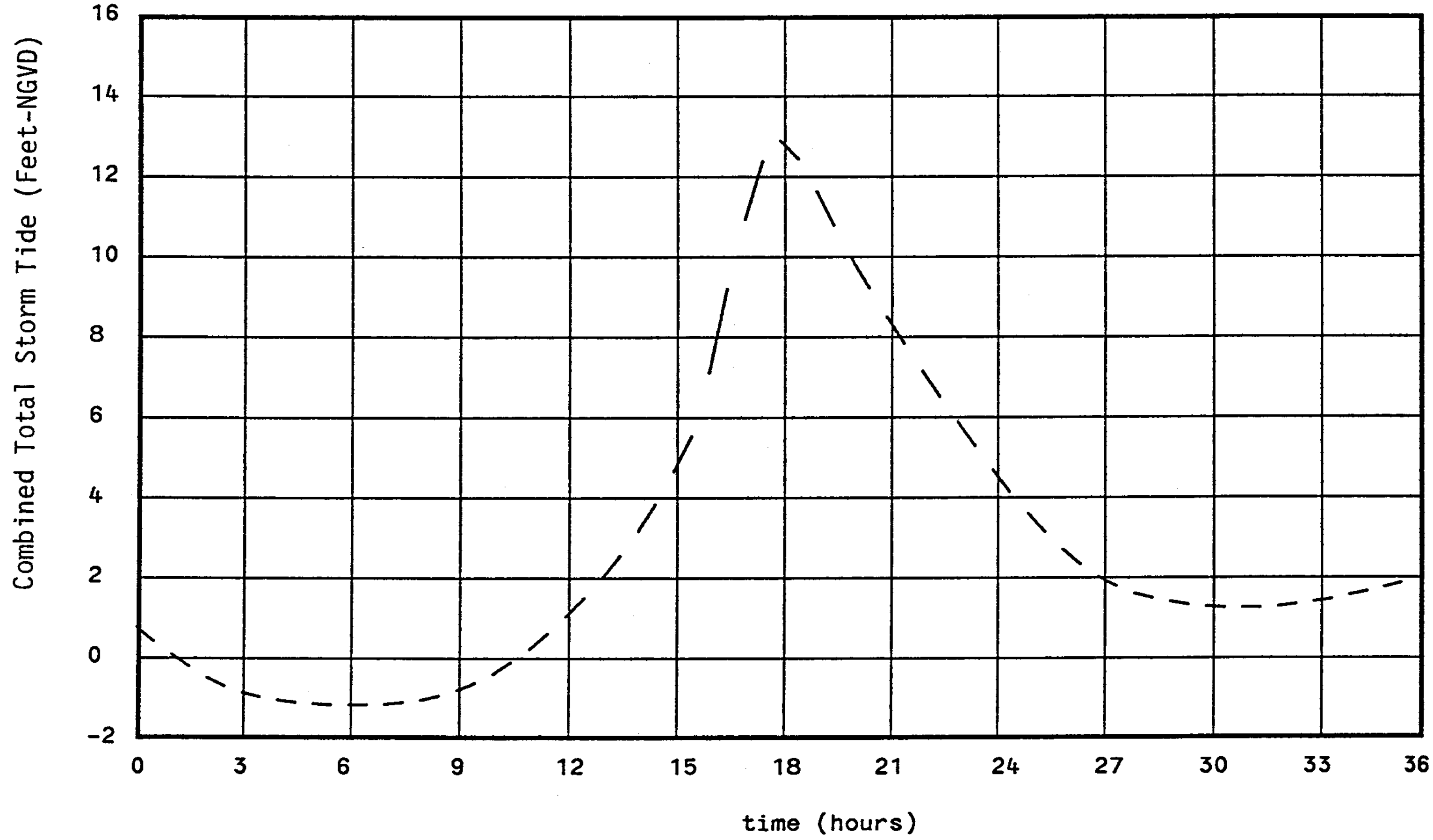

Figure CIII 100 Year Frequency Combined Total Storm Tide Hydrograph for South Profile